Subcritical transitions in the parallel-plate flow of viscoelastic fluids

DOCTORAALSCRIPTIE NATUURKUNDE

Timon Idema

Instituut-Lorentz voor Theoretische Fysica
Universiteit Leiden

Contents

Introduction

At first glance, it seems to be possible to classify the substances one encounters in normal-day life into two categories: solid and liquid ones. The theoretical physicist's favorite beverage coffee for instance is clearly a liquid, whereas the cup he drinks it from is often solid stone. The physicist may stir the coffee to speed up the solution of sugar into it, and notice a laminar flow in his cup. As he already knows, this flow is well-described by the famous Navier-Stokes equations [5].

However, if our physicist goes home and starts making a cake to serve at coffee the next day, he might notice the cake batter clinging to the spoon he is using to stir it with. Unlike his coffee (from which he extracts the spoon relatively clean), the batter climbs up on the spoon, displaying the 'rod climbing' behaviour first described by Weissenberg [10]. The batter does not only contain materials like water (which are described by the Navier-Stokes equations and do not exhibit rod climbing), but also polymers, making it a different kind of material. It is not a (Newtonian) liquid, but an example of what is called a viscoelastic fluid. Viscoelastic materials are neither liquids nor solids, but display in their behaviour some characteristics of both. The class of viscoelastic materials is large: from viscoelastic fluids (roughly speaking being solutions of polymers), which one would naively expect to behave more or less as a fluid, to glass and rubber, which seem to behave as solids.

In this thesis we study the behaviour of viscoelastic fluids. In the first chapter we make precise what they are and derive a set of model equations for them. We single out a specific one (the Oldroyd-B model) and give necessary characteristics of the viscoelastic fluids described by this specific model. Finally, we introduce the experimental setup and explain why the flow of these fluids has to have subcritical instabilities.

In chapter 2 we analyse the Oldroyd-B model and derive an amplitude equation for the parallel-plate setup. From this equation we can find whether the flow is laminar or has subcritical or supercritical instabilities. The coefficients of this equation can not be computed analytically, so we have to use numerical methods. They are described in chapter 3.

In chapter 4 we list the results of our numerical computations. For some part (the values for linear instability) we can compare them to those found by Öztekin and Brown [8]. However, it turns out that the behaviour of the viscoelastic fluid is actually nonlinear, giving instabilities which are different in nature from the ones found by linear stability analysis.

Chapter 1

Viscoelastic materials

1.1 Viscous and elastic

A liquid, such as water, generally has a nonzero viscosity (η), but no elasticity (μ). When we put a stress on a sample of liquid, it will therefore quickly adapt. The internal stress will shortly peak and then disappear completely (see figure 1.1).

To the contrary, a solid has a vanishing viscosity but a nonzero elasticity. It therefore reacts completely differently when put under stress. There will be a persistent internal stress (at a plateau which is reached in a time comparable to the duration of the peak in water) which in principle will remain forever (figure 1.2).

A viscoelastic material has both nonzero viscosity and nonzero elasticity. How it will react to stress depends on which of these is dominant. If the effect of the elasticity is larger than that of the viscosity, we call the material a liquid-like solid. When put under stress, the internal stress will reach a plateau like that of a solid, but which decreases (sometimes extremely) slowly (figure 1.3). An example is rubber.

If the viscosity is dominant, the material is termed a solid-like liquid. In this case the internal stress disappears after a characteristic relaxation time λ, which is large in comparison to the duration of the peak in a normal liquid, but much smaller then the timescale on which the plateau of a liquid-like solid disappears (figure 1.4). An example is a polymer solution in a liquid.

These solid-like liquid polymer solutions are our objects of study. We shall consider them to consist of a liquid solvent fluid (which we call a Newtonian fluid and is supposed to behave according to the Navier-Stokes equations) in which a polymer is dissolved. The thus obtained solution is what we call a viscoelastic fluid.

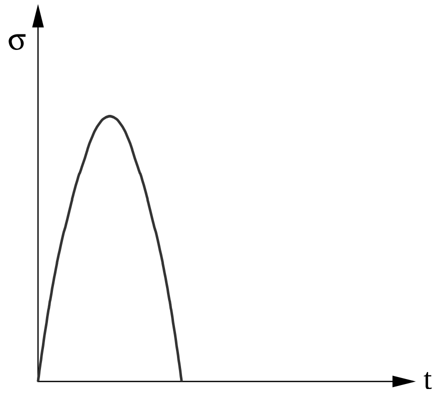

Figure 1.1: The stress of a liquid

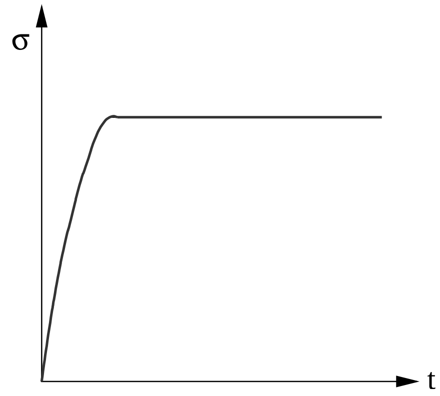

Figure 1.2: The stress of a solid

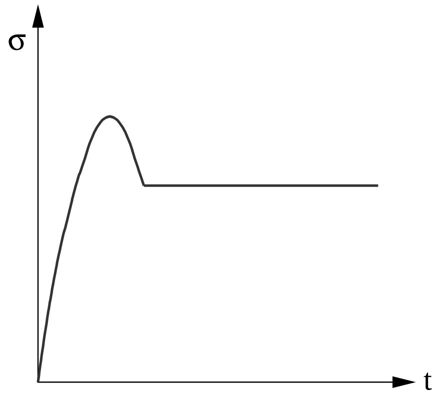

Figure 1.3: The stress of a liquid-like solid

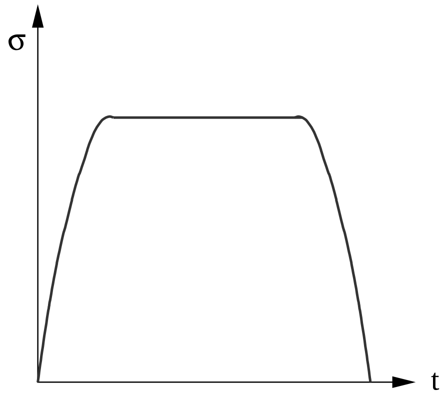

Figure 1.4: The stress of a solid-like liquid

1.2 A model for a viscoelastic fluid

To determine the stresses of the liquid and solid, we look at what happens if we apply an external stress to a sample of each (figure 1.5). If the stress is applied such that we get a displacement $u(x)$ in the positive y direction, the liquid will adapt depending on how fast this displacement moves, giving

$$\sigma^{(l)} = \eta \frac{\partial v}{\partial x} = \eta \frac{\partial}{\partial x} \frac{\partial u}{\partial t}.$$

For the solid however, the magnitude of the internal stress depends completely on the size of the displacement. It does not matter whether this displacement was created instantaneously or came to be over the course of thousands of years. The stress is therefore given by:

$$\sigma^{(s)} = \mu \frac{\partial u}{\partial x}.$$

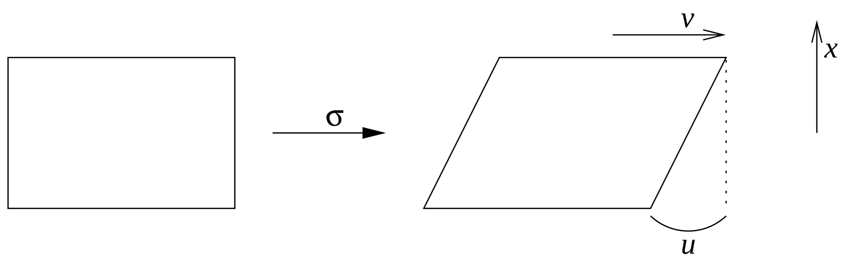

Figure 1.5: A sample put under stress

As stated in the previous section, viscoelastic materials have both solid-like ($\mu \neq 0$) and liquid-like ($\eta \neq 0$) characteristics. It is therefore sensible to consider their (internal) stress σ to have liquid $\sigma^{(l)}$ and solid $\sigma^{(s)}$ contributions.

As a model, we shall build a viscoelastic material out of solid and liquid building blocks. This heuristic approach will give us the equations of the Oldroyd-B model. For a more formal approach based on tensor calculus, see [1].

We graphically represent the solid and liquid building blocks as follows:

solid	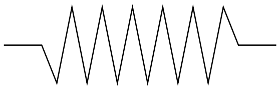	$\mu \neq 0$	$\sigma = \mu \frac{\partial u}{\partial x}$
liquid	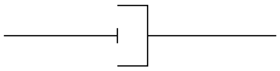	$\eta \neq 0$	$\sigma = \eta \frac{\partial}{\partial t} \frac{\partial u}{\partial x}$

We combine these building blocks as resistors would be in an electric circuit. Since this results in a flow circuit, we can apply Kirchhoff's laws to them. These laws tell us how to combine the displacements and stresses of the individual building blocks to find those of the full circuit.

The two simplest linear combinations are:

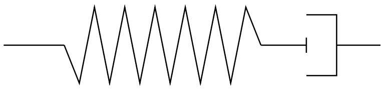	$u = u_1 + u_2$ $\sigma = \sigma_1 = \sigma_2$	solid-like liquid	Maxwell model
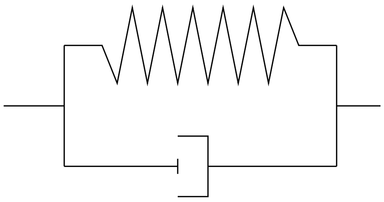	$u = u_1 = u_2$ $\sigma = \sigma_1 + \sigma_2$	liquid-like solid	Kelvin model

We can find an equation for σ for these and all other combinations of the two building blocks by simply using Kirchhoff's laws and using the expressions linking σ and u that we have for either block. This gives us a model equation for the behaviour of each viscoelastic material for which we can build such a circuit. Our material behaves as the simple solid-like liquid in the first row, which is sometimes referred to as the 'dumbbell' (see section 1.3). Using $u = u_1 + u_2$ and $v = \frac{\partial u}{\partial t}$, we find for this system (the Maxwell model)

$$\sigma + \lambda_M \frac{\partial \sigma}{\partial t} = \eta \frac{\partial v}{\partial x}, \tag{1.1}$$

where

$$\lambda_M \equiv \frac{\eta}{\mu}. \tag{1.2}$$

However, we should be careful when taking the time derivative of σ. The stress is not only a function of time, but also of the location in the fluid. Since our fluid is moving, there is a nonzero 'convective contribution' to the total time derivative of σ. To find what it is, we first look at a scalar field $A(t, \vec{r})$ defined in the fluid. Using the chain rule, we find for the so-called convective derivative of A:

$$\frac{DA}{Dt} = \frac{\partial A}{\partial t} + \frac{\partial A}{\partial \vec{r}} \cdot \frac{\partial \vec{r}}{\partial t} = \frac{\partial A}{\partial t} + \frac{\partial A}{\partial \vec{r}} \cdot \vec{v} = \frac{\partial A}{\partial t} + \vec{v} \cdot \vec{\nabla} A.$$

For a vector the convective derivative is found analogous to that of a scalar field. For a tensor however, we find an extra contribution due to the fact that the principle axes of the tensor rotate and stretch over time. The convective derivative then becomes

$$\frac{D \overleftrightarrow{\sigma}}{Dt} = \frac{\partial \overleftrightarrow{\sigma}}{\partial t} + \vec{v} \cdot \vec{\nabla} \overleftrightarrow{\sigma} - \left(\vec{\nabla} \vec{v}\right)^{\dagger} \cdot \overleftrightarrow{\sigma} - \overleftrightarrow{\sigma} \cdot \left(\vec{\nabla} \vec{v}\right). \tag{1.3}$$

It is this derivative we should use in the Maxwell model (1.1). In tensor form it becomes the Upper-Convected Maxwell (UCM) model

$$\overleftrightarrow{\sigma} + \lambda_M \frac{D \overleftrightarrow{\sigma}}{Dt} = \eta \left[\vec{\nabla} \vec{v} + \left(\vec{\nabla} \vec{v}\right)^{\dagger}\right]. \tag{1.4}$$

The UCM model describes the behaviour of the polymers in our viscoelastic fluid. In the Oldroyd-B model, we also include the Newtonian solvent fluid. The total stress is simply the sum of the stresses of the polymer and the solvent:

$$\overleftrightarrow{\sigma} = \overleftrightarrow{\sigma}_p + \overleftrightarrow{\sigma}_s = \overleftrightarrow{\sigma}_p - \eta_s \left[\vec{\nabla} \vec{v} + \left(\vec{\nabla} \vec{v}\right)^{\dagger}\right]. \tag{1.5}$$

The Navier-Stokes equations now give

$$\rho \left[\frac{\partial \vec{v}}{\partial t} + \left(\vec{v} \cdot \vec{\nabla}\right) \vec{v}\right] = -\vec{\nabla} p - \vec{\nabla} \cdot \overleftrightarrow{\sigma}, \tag{1.6}$$

where the polymeric stress tensor satisfies the UCM equation (1.4)

$$\overleftrightarrow{\sigma}_p + \lambda_M \left[\frac{\partial \overleftrightarrow{\sigma}_p}{\partial t} + \vec{v} \cdot \vec{\nabla} \overleftrightarrow{\sigma}_p - \left(\vec{\nabla} \vec{v}\right)^{\dagger} \cdot \overleftrightarrow{\sigma}_p - \overleftrightarrow{\sigma}_p \cdot \left(\vec{\nabla} \vec{v}\right)\right] = -\eta_p \left[\vec{\nabla} \vec{v} + \left(\vec{\nabla} \vec{v}\right)^{\dagger}\right]. \tag{1.7}$$

Together, equations (1.5), (1.6) and (1.7) form the Oldroyd-B model.

1.3 Boger fluids

The Oldroyd-B model only correctly describes polymer solutions of which the polymers behave as the simple dumbbell used to derive the UCM equation in the previous section. There is a class of viscoelastic fluids that is especially prepared to behave as such. These are called Boger fluids. In this section we shall look at them more closely.

Suppose we do a plane-Couette-flow experiment with a Boger fluid. This means that we put the fluid between two (infinitely long) parallel plates a distance $2d$ apart. One of the plates moves with a velocity v_0 in the positive x direction and the other one moves with the same velocity in the negative x direction (figure 1.6). We set out to find the laminar flow and the associated total stress tensor.

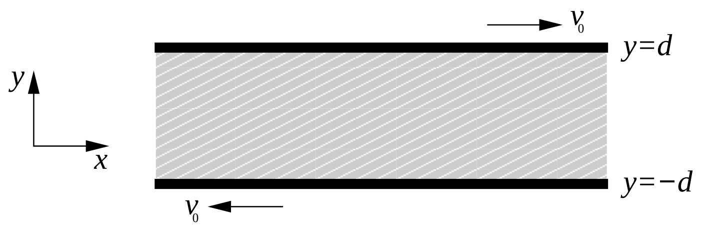

Figure 1.6: Couette flow

There is no force driving the fluid in the y or z direction, so the velocity has only a nonzero component in the x direction. Because the whole system is invariant under translations over x and z, the velocity and stress can be functions of y alone. This means that we have

$$\vec{v}(\vec{r}) = (v(y), 0, 0).$$

When we put this into the Navier-Stokes equations (1.6), we find that the left-hand side vanishes. The right-hand side then gives

$$\frac{\partial \sigma_{xy}}{\partial y} = 0. \tag{1.8}$$

From the equation for σ_p we get ($v' = \frac{\partial v}{\partial y}$)

$$\begin{aligned} \sigma_{xx} &= -2\eta_p \lambda (v')^2 \\ \sigma_{xy} &= -(\eta_p + \eta_s) v' \\ \sigma_{yy} &= \sigma_{xz} = \sigma_{yz} = \sigma_{zz} = 0. \end{aligned} \tag{1.9}$$

Combining equations (1.8) and (1.9), we find a differential equation for v:

$$\begin{cases} -(\eta_p + \eta_s) v'' &= 0 \\ v(\pm d) &= \pm v_0 \end{cases} \tag{1.10}$$

of which the solution is

$$v = \dot{\gamma} y, \qquad \text{with} \qquad \dot{\gamma} \equiv \frac{v_0}{d}, \tag{1.11}$$

and

$$\sigma_{xx} = -2\eta_p \lambda (\dot{\gamma})^2, \qquad \sigma_{xy} = -(\eta_s + \eta_p)\dot{\gamma}. \tag{1.12}$$

By 'experimental definition' the viscosity (η) is given by

$$\eta(\dot{\gamma}) \equiv -\frac{\sigma_{xy}(\dot{\gamma})}{\dot{\gamma}}. \tag{1.13}$$

Another useful quantity is the normal stress difference, which in this case is given by $\sigma_{xx} - \sigma_{yy}$. Using these definitions, we find that the Oldroyd-B model gives the following predictions for a Boger fluid:

1. $\eta = \eta_s + \eta_p$ and η is independent of $\dot{\gamma}$.

2. For the normal stress difference we have

$$\sigma_{xx} - \sigma_{yy} = -2\eta_p \lambda (\dot{\gamma})^2, \tag{1.14}$$

so the normal stress difference is quadratic in $\dot{\gamma}$ and by measuring it, we can determine the relaxation time λ.

1.4 Instabilities

As was pointed out in the introduction, a Newtonian fluid like water flows in a predictable and 'orderly' fashion. This kind of flow is called laminar flow, and it is also seen in a viscoelastic fluid if it moves slowly. However, if one drives a viscoelastic fluid too hard, this 'basic' laminar flow becomes unstable. In effect this means that it takes only a small perturbation of the basic flow to produce a completely different flow pattern, whereas for a slowly moving fluid a small perturbation just disappears after a relatively short time.

There are two kinds of such instabilities. The simplest one is a supercritical instability. To see what this is we take some parameter R that is related to the velocity of the fluid. We now plot the amplitude of the distortion that a small perturbation may cause in the supercritical case. This gives a graph like figure 1.7. There is one critical value R_c of our parameter which separates the stable and unstable region. For $R < R_c$ the laminar flow is stable and nothing interesting will happen. However, for $R > R_c$ the flow is unstable to any small perturbation, so it will almost immediately evolve to a different flow pattern.

There are also subcritical instabilities, for which there are two relevant values of our parameter (see figure 1.8). For $R < R_s$ the flow is still stable, and for $R > R_c$ it is still completely unstable. However, for $R_s < R < R_c$ the laminar flow is stable for very small perturbations (whose amplitude does not reach above the dashed line), but unstable for larger ones. This is called the subcritical region.

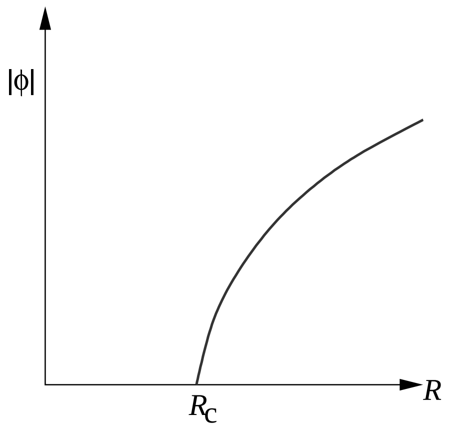

Figure 1.7: A supercritical instability

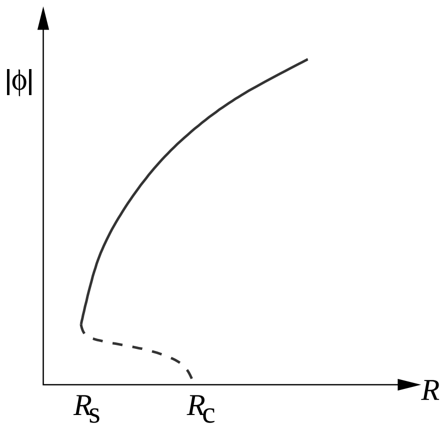

Figure 1.8: A subcritical instability

Using a simple argument which is due to Larson [6] we can see that the flow of a Boger fluid in a Taylor-Couette cell is unstable and that the instability is subcritical[1]. A Taylor-Couette cell consists of two concentrical cylinders. The space between the two cylinders is filled with the Boger fluid and the inner one is rotated with angular velocity Ω. The laminar flow can now be calculated in the same way as we did for the Couette flow; we find a curved flow in the azimuthal direction which is dependent on the radial position.

If we now consider a polymer which lies on such a curved flowline, we see that the outer part must move slightly faster than the inner part. This means that the outer part gets more stretched than the inner part, in effect bending the polymer. Because we found the normal stress difference to be nonzero (equation 1.14), this creates an inward force which is dependent on the angular velocity (see figure 1.9). For a certain value of the velocity this force becomes

[1]The same argument applies to the parallel-plate flow of section 1.5

larger than the friction and the polymer will start to move inward, deviating from the laminar flow. At this point the flow changes: we found an instability.

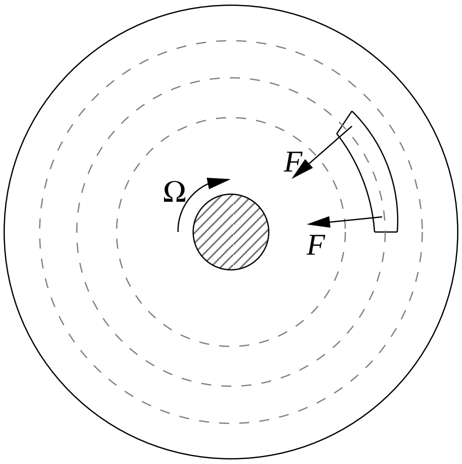

Figure 1.9: Instability in a Taylor-Couette cell

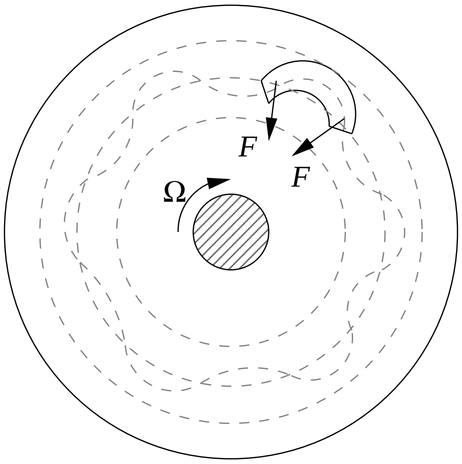

Figure 1.10: Second order instability

For velocities much smaller than this critical velocity, it seems that the polymer should neatly follow the laminar flow pattern. However, suppose that there is a relatively small, but relatively long-lived perturbation which looks like an oscillation on this flow line. Then locally the curvature of the (perturbed) flow line is much larger than that of the basic flow line, and a polymer that finds itself at such a point would experience an inward force large enough to start deviating from the laminar flow (figure 1.10). The flow is therefore stable to 'first order' perturbations, but not to 'second order' ones (i.e. perturbations upon perturbations). This means we are in the subcritical region.

1.5 The parallel-plate flow

The specific setup we study consists of two large parallel concentric disks. One is placed a distance H above the other. The viscoelastic fluid fills the volume between the two disks. One of the disks (which we take to be the lower one) is kept fixed, and the other one rotates with angular frequency Ω.

The natural coordinates to describe this system are cylindrical ones. The origin is positioned at the center of the lower disk. The whole configuration is shown in figure 1.11. The laminar flow between the two plates is sometimes referred to as parallel-plate flow.

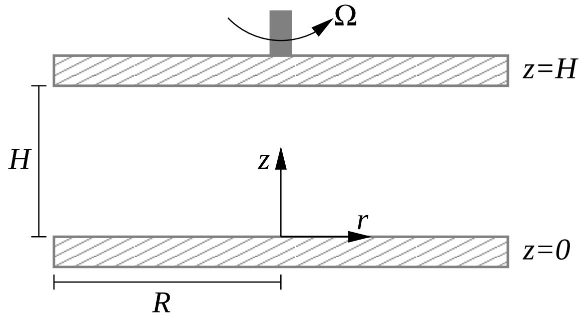

Figure 1.11: The parallel-plate setup

1.5.1 Variables and characteristics

In our calculations, we assume that the viscoelastic fluids used in the experiments behave as Boger fluids. We can therefore use the results from section 1.3. One of them is that the viscosity of the solvent η_s and that of the polymer η_p add up to give the total viscosity of the fluid $\eta_0 = \eta_s + \eta_p$.

The ratio

$$\beta \equiv \frac{\eta_s}{\eta_0} = \frac{\eta_s}{\eta_s + \eta_p} \tag{1.15}$$

will be used as a characteristic of the fluid. It is sometimes called the retardation parameter; its extremes $\beta = 0$ and $\beta = 1$ correspond to a Newtonian and a pure polymer ('Maxwellian') fluid.

Another characteristic of the Boger fluid is the relaxation time λ. Together with the rotation rate Ω it yields the dimensionless Deborah number

$$De \equiv \lambda\Omega, \tag{1.16}$$

which we shall use as a second parameter when describing the fluid[2].

We now introduce dimensionless variables

$$r \equiv \frac{r^*}{H}, \qquad t \equiv t^*\Omega, \qquad v \equiv \left(\frac{1}{\Omega H}\right) v^*, \qquad \tau \equiv (1-\beta)\frac{\sigma_p}{\eta_p \Omega}, \tag{1.17}$$

where the variables with asterisks are the ones with the ordinary dimensions, v is the velocity of the fluid and τ the (symmetric) polymer stress tensor. For the total dimensionless stress tensor defined above we have:

$$\tau_{\text{total}} \equiv \tau + \tau_s = \tau - \beta\left(\vec{\nabla}\vec{v} + \left(\vec{\nabla}\vec{v}\right)^\dagger\right). \tag{1.18}$$

We shall work with the dimensionless variables defined above throughout this thesis.

1.6 Earlier experimental and numerical results

For a long time, people believed that one could learn all there is to know about viscoelastic models by performing a linear stability analysis. Nonlinear effects were not taken into account because they were thought to be negligible. In 2000, Groisman and Steinberg were the first to deviate from this well-trodden path. In a Letter to Nature they reported experimental results that showed turbulence in the plate-plate flow of a low-Reynolds number viscoelastic fluid [4]. In contrast to Newtonian fluids (which only exhibit turbulence at high Reynolds number), they argued that it were the nonlinear mechanical properties of polymers that allowed turbulence to appear at arbitrarily low Reynolds number, because the role inertia plays in the Newtoinan fluid is taken over by elasticity in the polymer solution. From their experiments they concluded that for sufficiently high Weissenberg number, the elastic polymer solution they used showed all the main features of turbulence.

[2]Some authors prefer the Weissenberg number, denoted as Wi or We, and defined as $We \equiv \lambda\Omega R/H = De R/H$. Here R is the radius of the disks; the Weissenberg number is therefore simply the Deborah number multiplied with the aspect ratio.

In the same volume of Nature, Larson (an authority on the field) gave his view [6] on the letter of Groisman and Steinberg. He states that inertia has nothing to do with what he calls ‘polymeric turbulence’, because for polymer solutions higher viscosity gives a lower critical velocity for the onset of turbulence. This is completely opposite to the effect in inertially driven turbulence, where higher viscosity requires higher velocity to get instabilities. In this article Larson argues that the stretching of the polymers produces an inward radial pressure gradient, the effect that causes the ‘rod climbing’. On the other hand, inertial stresses (that occur at high velocity) generate a similar, but outward radial pressure gradient. Larson claims that it is this pressure gradient that causes the instability, both in the case where its source is inertia and where it is elasticity. (We used this explanation of the instability of a viscoelastic fluid in section 1.4).

In this thesis, we shall also focus on the nonlinear effects of our model. However, we will find the eigenfunctions and critical values of the linearized model along the way. Since this linearized model has been studied before, we can compare these results to the ones found earlier. In particular, we shall compare them to the numerical results obtained by Öztekin and Brown [8]. They in turn did their calculations in an attempt to explain experiments performed in 1991 by McKinley et al. [7]. In a combined effort, they produced new experimental and numerical results in 1994 [2], which already showed the flow to be subcritical in the rotation rate. However, they did not perform a nonlinear analysis to explain this subcritical instability.

Chapter 2

From model to amplitude equation

2.1 The complete model

In section 1.2 we introduced the Oldroyd-B model. It consists of two parts: the Navier-Stokes equations (1.6) for the whole fluid and a stress-equation for the polymeric part (1.7). Furthermore, to very good approximation, our fluid is incompressible, so we shall assume the following incompressibility condition to hold as well:

$$\vec{\nabla} \cdot \vec{v} = 0. \tag{2.1}$$

Equations (1.6) and (1.7) are not yet expressed in terms of the dimensionless variables we introduced in section 1.5. Translating to the new variable system, we find for the Navier-Stokes equations:

$$Re \left[\frac{\partial \vec{v}}{\partial t} + \left(\vec{v} \cdot \vec{\nabla} \right) \vec{v} \right] = -\vec{\nabla} p - \vec{\nabla} \cdot \overleftrightarrow{\tau} + \beta \Delta \vec{v}, \tag{2.2}$$

where the Reynolds number is defined as[1]

$$Re \equiv \frac{\Omega H^2 \rho}{\eta_s + \eta_p}. \tag{2.3}$$

Because we work with high viscosities, our Reynolds number is extremely small (whereas to get instabilities in a purely Newtonian fluid, one needs a large Reynolds number). To good approximation, this makes the left-hand side of equation (2.2) negligible. We therefore work with $Re = 0$.

The complete set of equations of our model in dimensionless variables is now given by

$$\vec{\nabla} \cdot \vec{v} = 0 \tag{2.4}$$

$$-\vec{\nabla} p - \vec{\nabla} \cdot \overleftrightarrow{\tau} + \beta \Delta \vec{v} = 0 \tag{2.5}$$

$$\overleftrightarrow{\tau} + De \left[\frac{\partial \overleftrightarrow{\tau}}{\partial t} + \vec{v} \cdot \vec{\nabla} \overleftrightarrow{\tau} - \left(\vec{\nabla} \vec{v} \right)^{\dagger} \cdot \overleftrightarrow{\tau} - \overleftrightarrow{\tau} \cdot \left(\vec{\nabla} \vec{v} \right) \right] = -\left(1 - \beta\right) \left(\left(\vec{\nabla} \vec{v} \right) + \left(\vec{\nabla} \vec{v} \right)^{\dagger} \right). \tag{2.6}$$

[1]More generally, the Reynolds number is defined as $Re \equiv VL\rho/\eta$ with V a characteristic velocity scale, L a characteristic length scale and ρ the density.

2.2 An exact solution

First we set out to find the steady-state solution of equations (2.4), (2.5) and (2.6) (to which we shall refer as the Oldroyd-B model from now on) in our particular setup. Because the whole system is symmetric under rotations over the azimuthal direction θ, the flow can only be a function of r and z and only move in the θ direction. We therefore have

$$\vec{v} = (0, v(r, z), 0). \tag{2.7}$$

Straightforward substitution then gives the following differential equation for v:

$$\left\{ \begin{array}{ccc} \frac{1}{r}\frac{\partial v}{\partial r} - \frac{v}{r^2} + \frac{\partial^2 v}{\partial r^2} + \frac{\partial^2 v}{\partial z^2} & = & 0 \\ v(r, 0) & = & 0 \\ v(r, 1) & = & r \end{array} \right. \tag{2.8}$$

Assuming $v(r, z)$ to be separable in r and z, we find the following solution

$$v(r, z) = rz. \tag{2.9}$$

The complete steady-state solution is given by

$$\vec{v} = (0, rz, 0) \tag{2.10}$$

$$\overleftrightarrow{\tau} = -(1-\beta)r \begin{pmatrix} 0 & 0 & 0 \\ 0 & 2Der & 1 \\ 0 & 1 & 0 \end{pmatrix} \tag{2.11}$$

$$p = -(1-\beta)Der^2. \tag{2.12}$$

2.3 Beyond the steady-state motion

The steady-state motion we found in the previous section describes the laminar flow between the two plates. It does not evolve over time and can be considered as an 'always present' basic flow. It is therefore rather uninteresting, and if we want to find patterns or evolution, we have to look beyond it. To be able to study the non-laminar flow, we write the total flow of the fluid as the sum of a laminar and a non-laminar part:

$$\mathbf{V}^{\text{total}} = \mathbf{V}^{\text{laminar}} + \mathbf{V}, \tag{2.13}$$

where $\mathbf{V}$ is a 10-dimensional vector which contains all the information of the system:

$$\mathbf{V} \equiv (v_r, v_\theta, v_z, p, \tau_{rr}, \tau_{r\theta}, \tau_{rz}, \tau_{\theta\theta}, \tau_{\theta z}, \tau_{zz})^{\mathrm{T}}. \tag{2.14}$$

We now put the vector $\mathbf{V}^{\text{total}}$ into the system ((2.4), (2.5), (2.6)). The terms which contain only $\mathbf{V}^{\text{laminar}}$ do of course yield the equations for the laminar flow and therefore cancel out. This leaves us with a set of equations which has terms that are either linear or quadratic in $\mathbf{V}$. Together, they can be written in the general form, combining the 10 equations (2.4), (2.5) and (2.6):

$$\hat{\mathcal{L}}\mathbf{V} + DeA\frac{\partial \mathbf{V}}{\partial t} = N(\mathbf{V}, \mathbf{V}), \tag{2.15}$$

where $\hat{\mathcal{L}}$ is a linear operator on $\mathbf{V}$, $N(\mathbf{V}, \mathbf{V})$ is a vector-valued bilinear operator on $\mathbf{V}$ and A is the 10×10 diagonal matrix given by

$$A = \text{diag}(0, 0, 0, 0, 1, 1, 1, 1, 1, 1).$$

Equation (2.15) is our central equation. Its components are written out in Appendix A.

2.4 The amplitude equation

Our objective is to get an equation for the amplitude of the non-laminar flow $\mathbf{V}$ from equation (2.15):

$$\hat{\mathcal{L}}\mathbf{V} + DeA\frac{\partial \mathbf{V}}{\partial t} = N(\mathbf{V}, \mathbf{V}).$$

For the eigenvalues and eigenfunctions of the (purely spatial) operator $\hat{\mathcal{L}}$ we write

$$\hat{\mathcal{L}}\mathbf{V}_0 = \lambda \mathbf{V}_0, \tag{2.16}$$

where $\mathbf{V}_0$ is a function dependent on spatial variables only[2]. Equation (2.16) is in general not separable. We therefore need an extra assumption.

We take $\mathbf{V}$ as a function of r alone to behave as a damped oscillator, with a high amplitude close to the center of rotation and a lower one further out. If we look at some relatively large value R of the dimensionless radius, this oscillation has the form of a sine in a neighbourhood of R (see figure 2.1). For $r = R + \Delta r$ we can then write the r-dependence of $\mathbf{V}$ as a single Fourier mode, so $\mathbf{V}(r, \theta, z) = e^{i\alpha r}\mathbf{V}(\theta, z)$. Here α is the radial wave number which can take on any nonnegative real value. This approximation works well as long as r stays close to R, which we assume implicitly from now on[3].

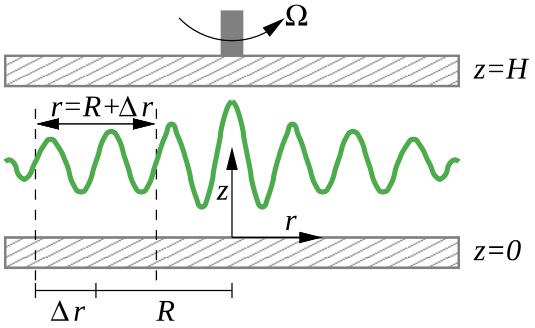

Figure 2.1: If we stay away from the center and from the outer edge, we can locally approximate the perturbation as a single Fourier mode in r. This approximation is valid in the region around $r = R$ that is indicated by the dashed lines. For any point in this region we write the radial coordinate as $r = R + \Delta r$.

It now makes sense also to take the θ-dependence to be a single Fourier mode and write

$$\mathbf{V}(r, \theta, z) = e^{i\alpha r} e^{im\theta}\mathbf{V}(z), \tag{2.17}$$

where the azimuthal wave number m is any integer. The form (2.17) allows for two types of functions: axisymmetric ones (when $m = 0$) and spiral ones (when $m \neq 0$). We focus on the

[2] To get the linear time evolution of V_0, we linearize (2.15) by taking $N \equiv 0$. This gives $\hat{\mathcal{L}}\mathbf{V}_0(\vec{r}, t) + \frac{\partial \mathbf{V}_0(\vec{r}, t)}{\partial t} = 0$, so by (2.16) we have $\lambda \mathbf{V}_0(\vec{r}, t) + \frac{\partial \mathbf{V}_0(\vec{r}, t)}{\partial t} = 0$ and $\mathbf{V}_0(\vec{r}, t) = e^{-\lambda t}\mathbf{V}_0(\vec{r})$.

[3] This assumption gives us the shape of the radial component of our functions $\mathbf{V}$, but also limits its range. A consequence is that we no longer have boundary conditions at the extrema of r. After all, we now stay away from both the center and the outer edge (which we theoretically can take to be at infinity).

axisymmetric case. Nonlinear flows with that shape have recently been found experimentally in the group of Larson. For the eigenfunctions of $\hat{\mathcal{L}}$ we can then write

$$\mathbf{V}_0 = \mathbf{V}_0(\vec{r}) = e^{i\alpha r} u_0(z). \tag{2.18}$$

As a trial solution of (2.15) we now use the Ansatz

$$\mathbf{V}(\vec{r},t) = \phi(t) e^{i\alpha r} u_0(z) + \phi^*(t) e^{-i\alpha r} u_0^*(z) + U_{\text{slaved}}, \tag{2.19}$$

where

$$U_{\text{slaved}} \equiv \sum_{n=2}^{\infty} \left[V_n e^{i\alpha r} + V_n^* e^{-i\alpha r} \right] + V_0, \tag{2.20}$$

and

$$\begin{array}{rcl} V_0 & = & |\phi|^2 u_0^{(2)} + |\phi|^4 u_0^{(4)} + |\phi|^6 u_0^{(6)} + \ldots \\ V_2 & = & \phi^2 u_2^{(2)} + \phi^2 |\phi|^2 u_2^{(4)} + \phi^2 |\phi|^4 u_2^{(6)} + \ldots \\ V_3 & = & \phi^3 u_3^{(3)} + \phi^3 |\phi|^2 u_3^{(5)} + \ldots \\ \text{etc.} & & \end{array}$$

The functions $u_i^{(j)}$ will be determined later.

Substitution of (2.19) into (2.15) yields an equation for the amplitude ϕ:

$$\begin{array}{rl} \left[\dfrac{\partial \phi}{\partial t} + \lambda \phi \right] e^{i\alpha r} u_0 & + \left[\dfrac{\partial \phi^*}{\partial t} + \lambda \phi^* \right] e^{-i\alpha r} {u_0}^* + \dfrac{\partial U_{\text{slaved}}}{\partial t} + \hat{\mathcal{L}} U_{\text{slaved}} \\ & = \phi^2 N(e^{i\alpha r} u_0, e^{i\alpha r} u_0) + (\phi^*)^2 N(e^{-i\alpha r} u_0^*, e^{-i\alpha r} u_0^*) \\ & \quad + |\phi|^2 \left[N(e^{i\alpha r} u_0, e^{-i\alpha r} u_0^*) + \rightleftarrows \right] \\ & \quad + \phi \left[N(e^{i\alpha r} u_0, U_{\text{slaved}}) + \rightleftarrows \right] \\ & \quad + \phi^* \left[N(e^{-i\alpha r} u_0^*, U_{\text{slaved}}) + \rightleftarrows \right] \\ & \quad + N(U_{\text{slaved}}, U_{\text{slaved}}), \end{array} \tag{2.21}$$

where $\rightleftarrows$ means that we take the previous term with the arguments interchanged.

To get an equation for the amplitude ϕ of $\mathbf{V}$ from (2.21), we need to 'select' the $e^{i\alpha r}$ Fourier-mode from it. This we can do using the following inner product, which is defined on the 10-dimensional space H that consists of all possible vectors[4] $\mathbf{V}$:

$$\langle \mathbf{U}, \mathbf{V} \rangle \equiv \left(\frac{\alpha}{2\pi} \right) \int_0^{\frac{2\pi}{\alpha}} dr \left(\frac{1}{2\pi} \right) \int_0^{2\pi} d\theta \int_0^1 dz \, (\mathbf{U}, \mathbf{V}), \tag{2.22}$$

where $(\mathbf{U}, \mathbf{V})$ is the Euclidean inner product of the vectors $\mathbf{U}$ and $\mathbf{V}$.

[4]Since the components of $\mathbf{V}$ are functions of r, θ and z, which are mappings to $\mathbb{C}$ from $D_1 = \mathbb{R}_+$, $D_2 = [0, 2\pi]$ and $D_3 = [0, 1]$ respectively, this general definition makes H a product of ten infinite-dimensional function spaces. Each of these function spaces consists of mappings from $D \equiv D_1 \times D_2 \times D_3$ into $\mathbb{C}$. However, for the variables r and θ we restrict ourselves to the mappings which can be written as Fourier modes, for which the integrals in (2.22) exist. To make sure the inner product is well-defined, we should restrict the functions of z to square-integrable functions over D_3. This means that, after performing the integrations over r and θ (which yield finite complex numbers), we should be left with a space which is isomorphic to the Hilbert space $L^2([0, 1], \mathbb{C})$.

We define the adjoint operator $\hat{\mathcal{L}}^+$ of $\hat{\mathcal{L}}$ by demanding that it satisfies

$$\left\langle \mathbf{U}, \hat{\mathcal{L}}\mathbf{V} \right\rangle = \left\langle \hat{\mathcal{L}}^+\mathbf{U}, \mathbf{V} \right\rangle . \tag{2.23}$$

The action of $\hat{\mathcal{L}}^+$ on $\mathbf{U}$ can be determined by partially integrating each of the ten components of (2.23). It is written out in appendix A. For its eigenvalues and eigenmodes we write[5]

$$\hat{\mathcal{L}}^+\mathbf{U}_0 = \eta U_0, \qquad U_0 = e^{-i\alpha r}\bar{m}(z). \tag{2.24}$$

Now using (2.22) to calculate the inner product of the adjoint mode with (2.21), we find an amplitude equation of the form

$$\frac{\partial \phi}{\partial t} = C_1\phi + C_3\phi|\phi|^2 + C_5\phi|\phi|^4 + \ldots \tag{2.25}$$

(for the explicit form, see appendix B).

Not surprisingly, we find to first order in ϕ:

$$\frac{\partial \phi}{\partial t} = -\lambda\phi, \tag{2.26}$$

so $C_1 = -\lambda$. To find C_3 and C_5 we need to go to third and fifth order in ϕ, which yields complicated but computable expressions. They involve the adjoint mode $\bar{m}(z)$ and several nonlinear modes $u_i^{(j)}$. All of these can be found from equation (2.15), using the numerical methods described in chapter 3. Again, explicit expressions are given in appendix B.

To get the behaviour of our system from the amplitude equation (2.25), we now look for solutions which are stable, i.e. $\frac{\partial \phi}{\partial t} = 0$. If we only go to third order, we find that they satisfy

$$|\phi|^2 = \frac{\lambda}{C_3}, \tag{2.27}$$

where λ and C_3 are the real parts of the numbers in (2.25). From this we see that there is only a solution if λ and C_3 have the same sign. This means that the third order contribution magnifies the effect of the linear term. To this order, we can therefore only find supercritical instabilities.

To fifth order however, we find nonzero stable amplitudes at

$$|\phi|^2 = \frac{-C_3 \pm \sqrt{C_3^2 + 4\lambda C_5}}{2C_5} \tag{2.28}$$

(where again λ, C_3 and C_5 are the real parts of the numbers in (2.25)). There are solutions if the right-hand side of (2.28) is positive. If both C_3 and C_5 have the same sign as λ, this enhances the supercritical behaviour found before. However, if in the region of linear stability we have $C_3 > 0$ and $C_5 < 0$, we can also get solutions from (2.28) that give a subcritical instability.

[5]Notice that the eigenvalues of $\hat{\mathcal{L}}^+$ are the same as those of $\hat{\mathcal{L}}$ and that the inner product of an eigenmode of $\hat{\mathcal{L}}$ and one of $\hat{\mathcal{L}}^+$ associated to different eigenvalues vanishes. That this is true can be seen immediately by taking an eigenmode $\mathbf{V}_0$ with eigenvalue λ of $\hat{\mathcal{L}}$ and an eigenmode $\mathbf{U}_0$ with eigenvalue η of $\hat{\mathcal{L}}^+$ and write:

$$\eta \left\langle \mathbf{U}_0, \mathbf{V}_0 \right\rangle = \left\langle \mathcal{L}^+\mathbf{U}_0, \mathbf{V}_0 \right\rangle = \left\langle \mathbf{U}_0, \mathcal{L}\mathbf{V}_0 \right\rangle = \lambda \left\langle \mathbf{U}_0, \mathbf{V}_0 \right\rangle ,$$

from which we find that either $\lambda = \eta$ or $\langle \mathbf{U}_0, \mathbf{V}_0 \rangle = 0$.

2.5 Computing eigenvalues and modes

To compute C_3 and C_5 in (2.25), we need to find the linear modes (eigenmodes of $\hat{\mathcal{L}}$), adjoint modes (eigenmodes of $\hat{\mathcal{L}}^+$) and several nonlinear modes (the functions $u_i^{(j)}$ from (2.20)). They can all be found from equation (2.15).

2.5.1 The linear and adjoint modes

To find the linear modes $\mathbf{V}_0$ and eigenvalues λ, we look at (2.15) with $N \equiv 0$. We use our earlier assumption that we can express the r and θ-dependence as a single Fourier mode, yielding for the axisymmetric mode ($m = 0$):

$$\mathbf{V}_0 = V_0(\vec{r}) = e^{i\alpha r} u_0(z).$$

When we put this into (2.16)

$$\hat{\mathcal{L}}\mathbf{V}_0 = \lambda \mathbf{V}_0,$$

we can extract equations for the velocity components v_r, v_θ and v_z by eliminating τ and p. Moreover we notice that the incompressibility condition (2.4) in this case links v_r and v_z by

$$v_r(z) = -\left(\frac{1}{r} + i\alpha\right)^{-1} \frac{\partial v_z(z)}{\partial z}. \tag{2.29}$$

Hence, we can also eliminate v_r from (2.15) and end up with two coupled differential equations for v_θ and v_z of the form

$$\frac{\partial^2 v_\theta}{\partial z^2} = A(r,\lambda)v_\theta(z) + B(r,\lambda)v_z(z) + C(r,\lambda)\frac{\partial^2 v_z(z)}{\partial z^2}, \tag{2.30}$$

$$\frac{\partial^4 v_z}{\partial z^4} = D(r,\lambda)v_\theta(z) + E(r,\lambda)\frac{\partial^2 v_\theta(z)}{\partial z^2} + F(r,\lambda)\frac{\partial^2 v_z(z)}{\partial z^2}. \tag{2.31}$$

The expressions for the coefficients are given in appendix A.

Because the perturbations to the laminar flow must vanish at the boundaries (the top and lower plate, located at $z = 0$ and $z = 1$) the boundary conditions for this system are given by

$$\vec{v}(z=0) = \vec{v}(z=1) = 0, \tag{2.32}$$

or explicitly (writing a prime for the derivative with respect to z and transforming v_r to v_z' using (2.29)):

$$\begin{array}{lll} v_\theta(0) = 0, & v_z(0) = 0, & v_z'(0) = 0, \\ v_\theta(1) = 0, & v_z(1) = 0, & v_z'(1) = 0. \end{array} \tag{2.33}$$

For a given value of λ, integration of (2.30, 2.31) gives the solution of the linear system (2.16). However, this eigenvalue must first be found, which means that we have a system with seven parameters and only six conditions. We therefore need an additional (normalization) condition on the system, which (from a mathematical point of view) we are free to choose. Physically, it makes sense to set the scale of the non-laminar flow to match that of the laminar flow. In that way, we can estimate the effect of a distortion by looking at the size of its amplitude $|\phi|$. To apply this scaling, we need to normalize the shear rate of the non-laminar flow, taking

$$\max\left|\frac{\partial v_\theta}{\partial z}\right| = 1. \tag{2.34}$$

We can now find λ and $\mathbf{V}$ as functions of De, α and R using the numerical methods described in the next chapter.

As remarked before, the eigenvalues of the adjoint operator are the same as those of the linear operator $\hat{\mathcal{L}}$. To find the adjoint eigenmodes, we proceed in exactly the same way as we did to find the linear ones. This also yields two coupled differential equations for two components of the 10-dimensional eigenvector $\mathbf{U}_0$. They are given, together with the expressions for the adjoint operator, in appendix A.

2.5.2 Nonlinear modes

The nonlinear modes $u_i^{(j)}$ are also solutions of (2.15), but with a nonzero right-hand side. By construction however, the function on the right-hand side only contains modes that we already know. To illustrate this, the expression for the mode $u_2^{(2)}$ (which is part of the $e^{2i\alpha r}$ Fourier mode) is given by

$$\hat{\mathcal{L}}\left(e^{2i\alpha r}u_2^{(2)}\right) - 2\lambda e^{2i\alpha r}u_2^{(2)} = N\left(e^{i\alpha r}u_0, e^{i\alpha r}u_0\right), \tag{2.35}$$

where λ is the eigenvalue of $\hat{\mathcal{L}}$ associated to the linear mode $e^{i\alpha r}u_0$.

From (2.35) we see that we can find $u_2^{(2)}$ in the same way as we found the linear modes u_0. The only difference is that in this case the right-hand side N of (2.15) is not identically zero, but it is a fully known function. Taking it along in the derivation of the differential equations ((2.30), (2.31)), we find a similar system for the nonlinear modes. It is this system of equations that is explicitly given in appendix A.

There is one special case in which we get different expressions for the nonlinear modes. This occurs when we look at modes for which $n = 0$, yielding the $e^{0i\alpha r}$ mode. In that case the mode becomes a function of the spatial coordinate z alone. This means that the velocity can no longer have a component in the z-direction[6]. We are therefore left with only two velocity components (v_r and v_θ) which are functions of the spatial coordinate z.

To find a system of differential equations for these modes, we need to start from (2.15) again. The procedure is completely the same as the one we used when looking for the equations for the linear mode. It again yields two coupled differential equations, but in this case they are both second-order. They too are given explicitly in appendix A.

[6] If it would have a component in the z-direction, and the flow was in the positive z-direction for some (r, θ, z_0), it would have to be in the positive z-direction for all sets of (r, θ, z_0). This means there would be a slice through our system at $z = z_0$ through which fluid only flows up, creating a higher density above and a lower one below. But this is in conflict with the incompressibility condition.

Chapter 3

Numerical methods

3.1 Introduction

In this chapter the numerical methods used are described. They work with an N-dimensional vector of functions which is denoted as $y(x)$. In our specific case, the functions of interest are the perturbations to the velocity profile and their derivatives to the variable z, which we write as $v_r(z)$, $v_\theta(z)$, $v_z(z)$ and $v_r'(z)$, $v_\theta'(z)$, $v_z'(z)$. The boundary conditions on these are given by the requirement that all perturbations vanish at both plates, or, after rescaling, at both sides of the interval $[0, 1]$.

In the case where the radial wave number α is not zero, we have used the incompressibility condition to write v_r in terms of v_z'. We then found two coupled differential equations for v_θ'' and $v_z^{(\mathrm{IV})}$. In the programs these are translated into the vector y using the following convention:

$$y = \begin{pmatrix} v_\theta \\ v_\theta' \\ v_z \\ v_z' \\ v_z'' \\ v_z''' \end{pmatrix}.$$

This means we work with a 6-dimensional vector. The boundary conditions are translated into the requirement that the first, third and fourth component are equal to zero at both sides of the interval.

In the special case where $\alpha = 0$ we found that we always have $v_z(z) \equiv 0$. In that case we work with a 4-dimensional vector y:

$$y = \begin{pmatrix} v_r \\ v_r' \\ v_\theta \\ v_\theta' \end{pmatrix}.$$

The boundary conditions now state that the first and third component of y must vanish at both sides of the interval.

The relevant part of the C-code of the algorithms described below is given in appendix C.

3.2 RK4

The first program we need is an algorithm to 'integrate' ordinary differential equations. To do this we use the fourth-order Runge-Kutta method, which is famous for its accuracy and reliability. The code of both this algorithm and that of the shooting method described in the next section are based on similar algorithms given in [9].

The method works with a system of N coupled first-order differential equations, all of the general form

$$\frac{dy_i(x)}{dx} = f_i(x, y_1, \ldots, y_N) \qquad i = 1, \ldots, N, \tag{3.1}$$

where the functions f_i on the right-hand side are given by our problem.

The simplest integration algorithm advances a solution from x_n to $x_{n+1} \equiv x_n + h$ using the formula

$$y_{n+1} = y_n + hf(x_n, y_n) + \mathcal{O}(h^2), \tag{3.2}$$

with y_n the vector $(y_1(x_n), \ldots, y_N(x_n))$. This is known as the Euler method, but could also be called the first-order Runge-Kutta method. Unfortunately, it has a relatively large error of order h^2, which makes this method unappealing in comparison to others.

A somewhat more advanced algorithm is the midpoint or second-order Runge-Kutta method. It uses not just one, but two Euler-type steps to advance over a distance h:

$$\begin{aligned} k_1 &= hf(x_n, y_n) \\ k_2 &= hf(x_n + \frac{1}{2}h, y_n + \frac{1}{2}k_1) \\ y_{n+1} &= y_n + k_2 + \mathcal{O}(h^3). \end{aligned} \tag{3.3}$$

In effect, we first take a trial step and use the information gained to get a better estimate of the true value at the endpoint, reducing the error by one order. However, the accuracy would still increase if we also use information from a (trial) endpoint. This is done in the fourth-order Runge-Kutta method, which has four point evaluations: one at the start, one at a trial endpoint, and two at trial midpoints:

$$\begin{aligned} k_1 &= hf(x_n, y_n) \\ k_2 &= hf(x_n + \frac{1}{2}h, y_n + \frac{1}{2}k_1) \\ k_3 &= hf(x_n + \frac{1}{2}h, y_n + \frac{1}{2}k_2) \\ k_4 &= hf(x_n + h, y_n + k_3) \\ y_{n+1} &= y_n + \frac{k_1}{6} + \frac{k_2}{3} + \frac{k_3}{3} + \frac{k_4}{6} + \mathcal{O}(h^5). \end{aligned} \tag{3.4}$$

It is this method which turns out to have the best balance between accuracy and efficiency for practical use. It is implemented in the function `rk4`, which uses the function `derivs` to evaluate the right-hand side of (3.4). Both the shooting and the re-orthonormalization algorithms use this algorithm for integration.

3.3 Shooting

Numerically solving a system of ordinary differential equations which has boundary conditions at only one point (say $x = 0$) is simple and straightforward. One simply sets the functions to fit the boundary conditions at $x = 0$ and integrates over small steps, using an integration algorithm like RK4. This procedure immediately produces the solution $y(x)$ at any point x.

In our case not all the boundary conditions are given at the same point: some (say n_1) are set at $x = 0$, and the rest (say $n_2 = N - n_1$, with N the dimension of y) at $x = 1$. This presents us with a serious problem, because the input of our integration algorithm is the value of the function y at a single point x. However, only some components of y are fixed at either end of the interval.

A possible way to solve this problem is by using the shooting technique. We first choose some values for the components unspecified at one end of the interval (we take $x = 0$ as the starting point). We take the thus obtained fully specified starting vector $y(0)$ and integrate to $x = 1$. Next, the values of $y(1)$ this 'shot' has given are compared to the boundary conditions at $x = 1$. They will most likely be unsatisfied, but from the discrepancy we will be able to make a better guess for the freely chosen components at $x = 0$. After several shots, we thus obtain a solution that fits the boundary conditions at both sides.

The freely chosen components of $y(0)$ form an n_2-dimensional vector $\mathbf{V}$. At $x = 1$, we can write the discrepancies between the n_2 components of $y(1)$ and the boundary conditions as an n_2-dimensional vector $\mathbf{F}$. $\mathbf{F}$ is a function of $\mathbf{V}$ and the correct choice of $\mathbf{V}$ is of course the one which satisfies $\mathbf{F}(\mathbf{V}) = 0$. We search for this vector $\mathbf{V}$ using the Newton-Raphson root-finding method. Essentially, this means that we have to solve the following set of equations

$$\mathbf{J} \cdot \delta\mathbf{V} = -\mathbf{F}, \tag{3.5}$$

and then add the correction $\delta\mathbf{V}$ to our previous guess

$$\mathbf{V}^{\text{new}} = \mathbf{V}^{\text{old}} + \delta\mathbf{V}, \tag{3.6}$$

where the Jacobian $\mathbf{J}$ in (3.5) has components given by

$$J_{ij} = \frac{\partial F_i}{\partial V_j}. \tag{3.7}$$

The function `shoot` implements this method.

3.4 The re-orthonormalization method

There exists an alternative for the shooting method, which turns out to be very well suited for our specific problem. It is called the re-orthonormalization method and has several advantages if we compare it to the shooting method. One of them is that it can be programmed in such a way that we can compute all our desired functions (eigenvalues, linear, adjoint and nonlinear modes) with the same algorithm. Furthermore, once the linear eigenvalue and mode are found, we only need to make a single run for each nonlinear mode, whereas when using the shooting method, we essentially would have to start all over again. Finally, if we use the same number of integration steps, re-orthonormalization is more accurate than shooting. The method was first suggested by Godunov and later refined by Conte [3].

For this re-orthonormalization method, we need to write our boundary value problem in the following general form

$$
\begin{aligned}
y'(x) &= A(x)y(x) + f(x) && (3.8)\\
By(0) &= c_1 && (3.9)\\
Dy(1) &= c_2 && (3.10)
\end{aligned}
$$

where y and f are N-dimensional vectors, A is an $N \times N$ matrix, B is an $(N-k) \times N$ matrix of rank $N-k$, D a $k \times n$ matrix of rank k, c_1 a vector of $N-k$ components and c_2 one of k components. Equation (3.9) gives the boundary conditions at the starting point $x = 0$, equation (3.10) gives them at the endpoint $x = 1$. When looking for the linear modes, we take the inhomogeneous contribution $f(x)$ to be identically zero.

3.4.1 Analytical solution

Applying the principle of superposition, the solution of (3.8, 3.9) is found to be

$$
\begin{aligned}
y(x) &= y^{(0)}(x) + \beta_1 y^{(1)}(x) + \beta_2 y^{(2)}(x) + \ldots + \beta_k y^{(k)}(x)\\
&= y^{(0)}(x) + Y(x)\beta, && (3.11)
\end{aligned}
$$

where $y^{(0)}(x)$ is the solution of the inhomogeneous system

$$
\begin{aligned}
y'^{(0)}(x) &= A(x)y^{(0)}(x) + f(x) && (3.12)\\
By^{(0)}(0) &= c_1 && (3.13)
\end{aligned}
$$

and $Y(x)$ is an $n \times k$ matrix whose columns $y^{(1)}, \cdots, y^{(k)}$ are solutions of the homogeneous system

$$
\begin{aligned}
Y'(x) &= A(x)Y(x) && (3.14)\\
Y(0) &= U(0) && (3.15)
\end{aligned}
$$

with $U(0)$ again an $n \times k$ matrix with linearly independent columns that satisfies

$$BU(0) = 0. \qquad (3.16)$$

The solution (3.11) already satisfies the boundary conditions (3.9) at the start of the interval. Because it also needs to satisfy the conditions (3.10) at the end, we need to choose the constants $\beta = (\beta_1, \cdots, \beta_k)$ such that

$$Dy(1) = Dy^{(0)}(1) + DY(1)\beta = c_2. \qquad (3.17)$$

With this choice, we have an exact solution of our problem.

3.4.2 Numerical solution

Unfortunately, the analytical procedure to obtain the solution of our boundary value problem described above often gives incorrect or inaccurate results when we use numerical methods to find $y^{(0)}(x)$ and $Y(x)$. This is caused by the effect that the columns $y^{(1)}(x), \cdots, y^{(k)}(x)$ become less independent with increasing x, even though they start as linearly independent at

$x = 0$. This causes the matrix Y to be poorly conditioned at $x = 1$, where the elements of the vector β are determined. They will therefore be incorrect, and (3.11) does not produce the correct solution.

To prevent this effect of de-orthogonalisation of the column vectors of Y, we apply the trick suggested by Godunov. It is simply to re-orthonormalize the vectors at each integration step. If we carefully store the projections we use to realize this when advancing from $x = 0$ to $x = 1$, we can reconstruct the solution on the full interval using the one found at the endpoint.

As usual, we divide the integration interval $[0, 1]$ into m equal subintervals of length h. We integrate from x_{i-1} to x_i using the RK4-integration method described above. This yields the homogeneous solutions $Y(x_i)$ and the inhomogeneous solution $y^{(0)}(x_i)$. We then apply the Gramm-Schmidt process on $Y(x_i)$ to obtain an $n \times k$ matrix $Z(x_i)$ of orthonormal column vectors $z^{(1)}, \cdots, z^{(k)}$. Projection of $y^{(0)}(x_i)$ on the orthogonal complement of $Z(x_i)$ then yields a vector $z^{(0)}(x_i)$ which is orthogonal to each of the columns of $Z(x_i)$. The set $\left(z^{(0)}(x_i), Z(x_i)\right)$ obtained in this way can now be used as the basis for integration to x_{i+1}.

For later reconstruction of the true solution $y(x)$ we need to store the projections we use at each integration point. To facilitate this, we first observe that we can write the orthonormalization of $Y(x_i)$ to $Z(x_i)$ as the multiplication of Y with a $k \times k$ upper-triangular, nonsingular matrix $P^{(i)}$:

$$Z(x_i) = Y(x_i) P^{(i)}, \tag{3.18}$$

$$P^{(i)} = \begin{pmatrix} p_{11} & p_{12} & \cdots & p_{1k} \\ 0 & p_{22} & \cdots & p_{2k} \\ \vdots & \vdots & \ddots & \vdots \\ 0 & 0 & \cdots & p_{kk} \end{pmatrix}. \tag{3.19}$$

In our specific problem, we always work with $k = 2$ or $k = 3$. Since especially the formula for p_{1k} gets very complicated for large values of k, here only the result for $k \leq 3$ is given. The expressions for p_{ij} as given below are derived in appendix C.

Applying the Gramm-Schmidt process yields the following expressions for $z^{(i)}$:

$$\begin{aligned} w_{11} &= |y^{(1)}| \\ z^{(1)} &= \frac{y^{(1)}}{w_{11}} \end{aligned} \tag{3.20}$$

$$\begin{aligned} w_{22} &= |y^{(2)} - \left(y^{(2)}, z^{(1)}\right) z^{(1)}| \\ z^{(2)} &= \frac{y^{(2)} - \left(y^{(2)}, z^{(1)}\right) z^{(1)}}{w_{22}} \\ &= \frac{y^{(2)}}{w_{22}} - \frac{y^{(1)} \left(y^{(2)}, z^{(1)}\right)}{w_{11} w_{22}} \end{aligned} \tag{3.21}$$

$$\begin{aligned} w_{33} &= |y^{(3)} - \left(y^{(3)}, z^{(1)}\right) z^{(1)} - \left(y^{(3)}, z^{(2)}\right) z^{(2)}| \\ z^{(3)} &= \frac{y^{(3)} - \left(y^{(3)}, z^{(1)}\right) z^{(1)} - \left(y^{(3)}, z^{(2)}\right) z^{(2)}}{w_{33}} \\ &= \frac{y^{(3)}}{w_{33}} - \frac{y^{(1)} \left(y^{(3)}, z^{(1)}\right)}{w_{11} w_{33}} - \frac{y^{(2)} \left(y^{(3)}, z^{(2)}\right)}{w_{22} w_{33}} + \frac{y^{(1)} \left(y^{(2)}, z^{(1)}\right) \left(y^{(3)}, z^{(2)}\right)}{w_{11} w_{22} w_{33}} \end{aligned} \tag{3.22}$$

where

$$|y| = (y, y)^{\frac{1}{2}},$$

and for p_{ij}:

$$p_{ij} = 0 \qquad \text{for} \quad i > j \tag{3.23}$$

$$p_{ii} = \frac{1}{w_{ii}} \tag{3.24}$$

$$p_{12} = -\frac{\left(z^{(1)}, y^{(2)}\right)}{w_{11}w_{22}} \tag{3.25}$$

$$p_{23} = -\frac{\left(z^{(2)}, y^{(3)}\right)}{w_{22}w_{33}} \tag{3.26}$$

$$p_{13} = -\frac{\left(z^{(1)}, y^{(3)}\right)}{w_{11}w_{33}} + \frac{\left(z^{(1)}, y^{(2)}\right)\left(z^{(2)}, y^{(3)}\right)}{w_{11}w_{22}w_{33}}. \tag{3.27}$$

The projection of $y^{(0)}(x)$ on the space orthogonal to that spanned by the columns of $Z(x)$ is now straightforward and gives:

$$z^{(0)}(x_i) = y^{(0)}(x_i) - Z(x_i)\omega^{(i)}, \tag{3.28}$$

where $\omega^{(i)} = (\omega_{01}, \omega_{02}, \cdots, \omega_{0k})^{(i)}$ and

$$\omega_{0j} = \left(y^{(0)}, z^{(j)}\right) \qquad \text{for} \quad j = 1, \ldots, k. \tag{3.29}$$

We do not need to normalize the vector $z^{(0)}(x_i)$.

We write $U(x_{i+1}) = \left(u^{(1)}(x_{i+1}), \cdots, u^{(k)}(x_{i+1})\right)$ and $u^{(0)}(x_i)$ for the homogeneous and inhomogeneous solutions found by integration to the next mesh point. The information we need to store during our integration and re-orthonormalization ('forward') sweep are the matrices U and P and the vectors $u^{(0)}$ and ω at each integration point.

At the last point x_m we make a final orthonormalization, which yields $Z(x_m)$ and $z^{(0)}(x_m)$ in the same way as before. The 'real' solution $y(x_m)$ at the endpoint is then given by

$$y(x_m) = z^{(0)}(x_m) + Z(x_m)\beta^{(m)}, \tag{3.30}$$

where $\beta^{(m)}$ is the solution of the system

$$Dz^{(0)}(x_m) + DZ(x_m)\beta = c_2. \tag{3.31}$$

The function `godunovforward` carries out the forward sweep described above. When we are looking for the eigenvalues of our differential equations, we only need the eigenfunction y at the endpoint x_m to determine if it fits the boundary conditions at the end (see below). However, once we have found an eigenvalue, we do want to reconstruct the complete eigenfunction $y(x)$ on the full interval. Using the information we stored during the forward sweep, we can do this by a backward sweep using the solution found at the endpoint x_m.

If we know the solution at the point x_i $(1 \leq i \leq m)$, the solution at x_{i-1} is given by

$$y(x_{i-1}) = u^{(0)}(x_{i-1}) + U(x_{i-1})\beta^{(i-1)}, \tag{3.32}$$

where

$$\beta^{(i-1)} = P^{(i)}\left(\beta^{(i)} - \omega^{(i)}\right). \tag{3.33}$$

This backward sweep is made by the function `godunovbackward`.

3.4.3 Finding an eigenvalue

Before we can solve our nonlinear set of differential equations, we first need to solve a linear, homogeneous eigenvalue problem. Fortunately, the method described above can also be used to do this. In this section, the (temporal) eigenvalue of our problem will be denoted by σ and for the eigenfunction we have $y(x) = y(x, \sigma)$.

In the homogeneous case the function $f(x)$ in (3.8) is equal to zero. Therefore the inhomogeneous part $y^{(0)}(x)$ of the solution (3.11) will also vanish. In our specific case we are left with an homogeneous system in which $n = 6$ and $k = 3$:

$$y'(x, \sigma) = A(x, \sigma) y(x, \sigma). \tag{3.34}$$

The interval over which we integrate is $[0, 1]$. The boundary conditions are given by the requirement that the perturbations vanish at both boundaries, which translates to the following conditions on the vector y (y_j is the j^{th} component of the vector y):

$$\begin{array}{ccccccc} y_1(0) & = & y_3(0) & = & y_4(0) & = & 0, \\ y_1(1) & = & y_3(1) & = & y_4(1) & = & 0. \end{array} \tag{3.35}$$

However, there are now seven parameters to be fixed (we have a second and a fourth order differential equation and an eigenvalue). Only six of them are given by the boundary conditions, which means we need to add another one to get a unique solution. For this last condition we made the following (arbitrary) choice

$$v_z''(1) = 1, \tag{3.36}$$

or $y_5(1) = 1$.

Eventually, we do need a solution that is not based on this choice, but which is properly normalized. This is done by rescaling the homogeneous eigenfunction over the whole interval such that it satisfies

$$\max \left| \frac{dv_\theta}{dz} \right| = 1, \tag{3.37}$$

or, in terms of our vector y, that $\max |y_1(x)| = 1$ (see section 2.5.1).

We now take the following three orthonormal initial vectors $y^{(i)}$:

$$y^{(1)}(0) = \begin{pmatrix} 0 \\ 1 \\ 0 \\ 0 \\ 0 \\ 0 \end{pmatrix}, \qquad y^{(2)}(0) = \begin{pmatrix} 0 \\ 0 \\ 0 \\ 0 \\ 1 \\ 0 \end{pmatrix}, \qquad y^{(3)}(0) = \begin{pmatrix} 0 \\ 0 \\ 0 \\ 0 \\ 0 \\ 1 \end{pmatrix}, \tag{3.38}$$

and solve (3.34) for each of them, by making a forward sweep as described above. From (3.11) we now find the general solution to be

$$y(x) = \beta_1 y^{(1)}(x) + \beta_2 y^{(2)}(x) + \beta_3 y^{(3)}(x), \tag{3.39}$$

which already satisfies the boundary conditions at $x = 0$.

We now have to choose the β_i's and find σ such that we satisfy the four boundary conditions at $x = 1$. This gives us the following system which $\beta = (\beta_1, \beta_2, \beta_3)$ must satisfy:

$$\begin{array}{rcrcrcl} \beta_1 y_1^{(1)}(1,\sigma) & + & \beta_2 y_1^{(2)}(1,\sigma) & + & \beta_3 y_1^{(3)}(1,\sigma) & = & 0, \\ \beta_1 y_3^{(1)}(1,\sigma) & + & \beta_2 y_3^{(2)}(1,\sigma) & + & \beta_3 y_3^{(3)}(1,\sigma) & = & 0, \\ \beta_1 y_4^{(1)}(1,\sigma) & + & \beta_2 y_4^{(2)}(1,\sigma) & + & \beta_3 y_4^{(3)}(1,\sigma) & = & 0, \\ \beta_1 y_5^{(1)}(1,\sigma) & + & \beta_2 y_5^{(2)}(1,\sigma) & + & \beta_3 y_5^{(3)}(1,\sigma) & = & 1. \end{array} \tag{3.40}$$

The homogeneous system consisting of the first three equations of (3.40) has a solution exactly if the determinant of the coefficients vanishes. Once that is the case, these three equations give a solution $\beta = (\beta_1, \beta_2, \beta_3)$ of which one of the components is arbitrary. However, the system consisting of the first, second and fourth equation of (3.40) gives a unique solution β which also satisfies the third equation.

The determinant of the homogeneous system is a function of σ alone:

$$f(\sigma) = \begin{vmatrix} y_1^{(1)}(1,\sigma) & y_1^{(2)}(1,\sigma) & y_1^{(3)}(1,\sigma) \\ y_3^{(1)}(1,\sigma) & y_3^{(2)}(1,\sigma) & y_3^{(3)}(1,\sigma) \\ y_4^{(1)}(1,\sigma) & y_4^{(2)}(1,\sigma) & y_4^{(3)}(1,\sigma) \end{vmatrix} = 0. \tag{3.41}$$

To find a value of σ which satisfies (3.41), we use the Newton-Raphson root-finding technique. We take an initial guess σ_1 and a second guess $\sigma_2 = \sigma_1 + \varepsilon$, with $|\varepsilon| \ll |\sigma_1|$. Because $f(\sigma)$ is analytical in the neighbourhood of a true eigenvalue $\bar{\sigma}$, we can get a better approximation of $\bar{\sigma}$ using the recursion formula

$$\sigma_{i+1} = \sigma_i - \left(\frac{\sigma_i - \sigma_{i-1}}{f(\sigma_i) - f(\sigma_{i-1})} \right) f(\sigma_i). \tag{3.42}$$

Having found an eigenvalue σ, we solve (3.40) using Cramer's method and get the full eigenfunctions with the backward sweep. The procedure thus consists of several forward sweeps with trial eigenvalues σ_i until the function $f(\sigma)$ is sufficiently close to zero. A single backward sweep is then performed to get the complete eigenfunctions, which are essentially the velocity profiles. From these profiles it is a simple matter of substitution to find the stress profiles.

After we have found the linear (and adjoint) eigenfunctions (i.e. velocity profiles and stress profiles), we start looking for the nonlinear ones. To find them, we use the same procedure as for the linear ones, with some minor adjustments. In this case the eigenvalue σ is already found, so we only have to consider the six boundary conditions (3.35). This means the last equation of (3.40) is taken out. Furthermore, because we now have an inhomogeneous problem, the particular solution $y^{(0)}(x)$ comes into play and (3.40) gets a nonzero right-hand side:

$$\begin{array}{rcrcrcl} \beta_1 y_1^{(1)}(1) & + & \beta_2 y_1^{(2)}(1) & + & \beta_3 y_1^{(3)}(1) & = & -y_1^{(0)}(1), \\ \beta_1 y_3^{(1)}(1) & + & \beta_2 y_3^{(2)}(1) & + & \beta_3 y_3^{(3)}(1) & = & -y_3^{(0)}(1), \\ \beta_1 y_4^{(1)}(1) & + & \beta_2 y_4^{(2)}(1) & + & \beta_3 y_4^{(3)}(1) & = & -y_4^{(0)}(1). \end{array} \tag{3.43}$$

Finding one of the nonlinear functions is now a simple matter of making a forward sweep, finding the vector β from (3.43) and making a backward sweep.

Chapter 4

Results

4.1 Introduction

In this chapter, we present an overview of the results of the various numerical computations. First, we look at the linearized problem and search for the eigenvalues. For the least stable eigenvalue, we can compare our results with those obtained by Öztekin and Brown [8].

Having found the linear eigenvalues and modes, we turn to the full nonlinear problem. It turns out that some eigenvalues exhibit subcritical behaviour when we plot the amplitude as a function of De or R, whereas others are supercritical. Examples of both are shown in section 4.3.

When considered as functions of De, R, α and β, some eigenvalues even change from one type to the other. Naturally, also the size of the subcritical region is dependent on these parameters. For given De and β we look for the combinations of R and α that mark the transition to the linear instability and, if present, to the subcritical region. Some parts of the graphs obtained in this way turn out to follow a power law behaviour which can be found by looking at the asymptotic limit (taking $R \to \infty$). These results are presented in section 4.4.

4.2 Linear spectrum

First, we search for the eigenvalues and eigenfunctions of the operator $\hat{\mathcal{L}}$, which are solutions of equation (2.16):

$$\hat{\mathcal{L}}\mathbf{V}_0 = \lambda \mathbf{V}_0.$$

Following Öztekin and Brown, we choose our parameters to be $R = 5$, $\beta = 0.59$ and $\alpha = 3.5$. We look for the eigenvalues at Deborah numbers 1.0 - 5.0. Unlike Öztekin and Brown, we do not look only at the 'least stable' eigenvalue (i.e. the one with the largest real part), but also list the second, third and fourth one, since, as we will see in section 4.4, they also will play important roles. The numbers are given in table 4.1. In figure 4.1 we also plot the real against the imaginary part of the eigenvalues that belong to $De = 1.0$. We see that the 'higher' eigenvalues tend to get closer together and almost form a continuum.

Öztekin and Brown also give plots for the velocity and stress profiles of the linear mode at the point where it just becomes linearly unstable (i.e. the point where the real part of the least stable eigenvalue is zero). The parameters in this case are $De = 3.0$, $R = 2.3$, $\beta = 0.59$ and $\alpha = 3.5$. Our plots are given in figures 4.2 and 4.3. In these figures, the solid curves

De	Found eigenvalues	Öztekin and Brown
1.0	$-0.508641 - 0.445808i$	$-0.52 - 0.462i$
	$-0.583298 - 0.368102i$	
	$-0.678895 - 0.283834i$	
	$-0.729691 - 0.238155i$	
2.0	$-0.021489 - 0.425117i$	$-0.04 - 0.441i$
	$-0.092569 - 0.351973i$	
	$-0.183823 - 0.272483i$	
	$-0.232802 - 0.229616i$	
3.0	$0.134298 - 0.414694i$	$0.11 - 0.431i$
	$0.065491 - 0.343078i$	
	$-0.022757 - 0.265295i$	
	$-0.070186 - 0.223653i$	
4.0	$0.209441 - 0.408774i$	(none given)
	$0.142016 - 0.337779i$	
	$0.055703 - 0.260673i$	
	$0.009371 - 0.219599i$	
5.0	$0.253216 - 0.405083i$	$0.24 - 0.422i$
	$0.186677 - 0.334373i$	
	$0.101654 - 0.257546i$	
	$0.056098 - 0.216755i$	

Table 4.1: The first four axisymmetric eigenvalues for $R = 5.0$, $\beta = 0.59$ and $\alpha = 3.5$.

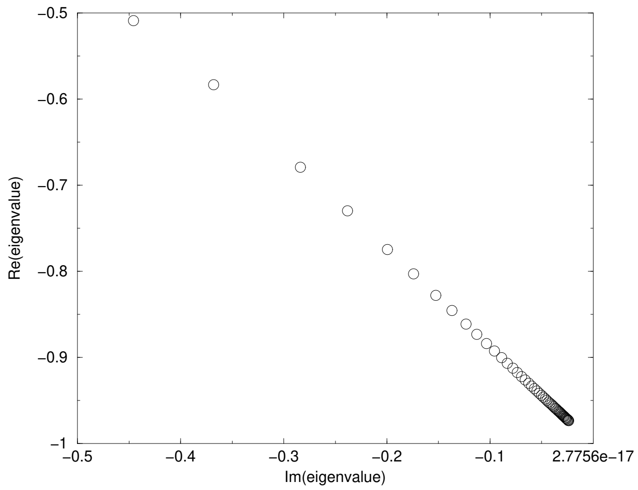

Figure 4.1: The real and imaginary parts of the eigenvalues for $De = 1.0$, $R = 5.0$, $\beta = 0.59$ and $\alpha = 3.5$.

are the real parts and the dashed curves the imaginary parts. Up to scaling factors and sign conventions, they are the same as those found by Öztekin and Brown.

4.3 Subcritical and supercritical instabilities

Not all eigenvalues exhibit the same behaviour around instability. A beautiful example is the first two eigenvalues which belong to the parameters $De = 2.0$, $\beta = 0.59$ and $\alpha = 6.0$. We have plotted the amplitude of the perturbation as a function of R in figures 4.4 and 4.5. The values of $|\phi|$ that are found are the stationary points of the amplitude equation (2.25)

$$\frac{\partial \phi}{\partial t} = C_1\phi + C_3\phi|\phi|^2 + C_5\phi|\phi|^4 + \dots$$

The dashed line shows what happens if we take only the C_3 contribution into account (so we go only to order ϕ^3). For the solid line we also used C_5 (and hence went to order ϕ^5).

From the graph showing a subcritical instability (figure 4.5), we see that in this case the subcritical region (the region between the onset R_s of the subcritical instability and that of total instability (R_c)) is about 3% of R_c. The amplitude of the non-laminar flow is 10-20% of that of the laminar flow. This is not very large, but it is a measurable effect.

4.4 Critical combinations

The interesting question is now of course how the values of R_c and R_s change as we vary the parameters of our system. We keep the value of β fixed at 0.59, so we constantly work with the same fluid. For fixed values of De we plot R_s and R_c as a function of the radial wave number α. This we do for the 'first four' eigenvalues. The results for Deborah numbers 2.0, 3.0 and 4.0 are plotted in figures 4.6, 4.7 and 4.8. The open circles, joined by solid lines, represent R_c, the filled diamonds, joined by dashed lines, give R_s in case the instabilities are subcritical. The minima, that is the smallest combination of R and α for which we first find an instability, are listed in table 4.2 for both the supercritical and the subcritical case.

One immediately notices that the notion of the 'first' or 'second' eigenvalue is not well-defined, because the R_c lines cross. The 'third' and 'fourth' eigenvalues are intertwined in a similar way. We have found no indication that these four eigenvalues mingle further among each other or that an even higher eigenvalue might come into play.

The subcritical region is relatively larger for bigger values of De. However, these plots do not all have the same vertical scale. Because R_c gets smaller as De increases, the absolute size of the subcritical region actually decreases with increasing De. That this is indeed the case can be seen in figure 4.9, where we plot the 'first two' eigenvalues of $De = 2.0$, $De = 3.0$ and $De = 4.0$ in a single picture.

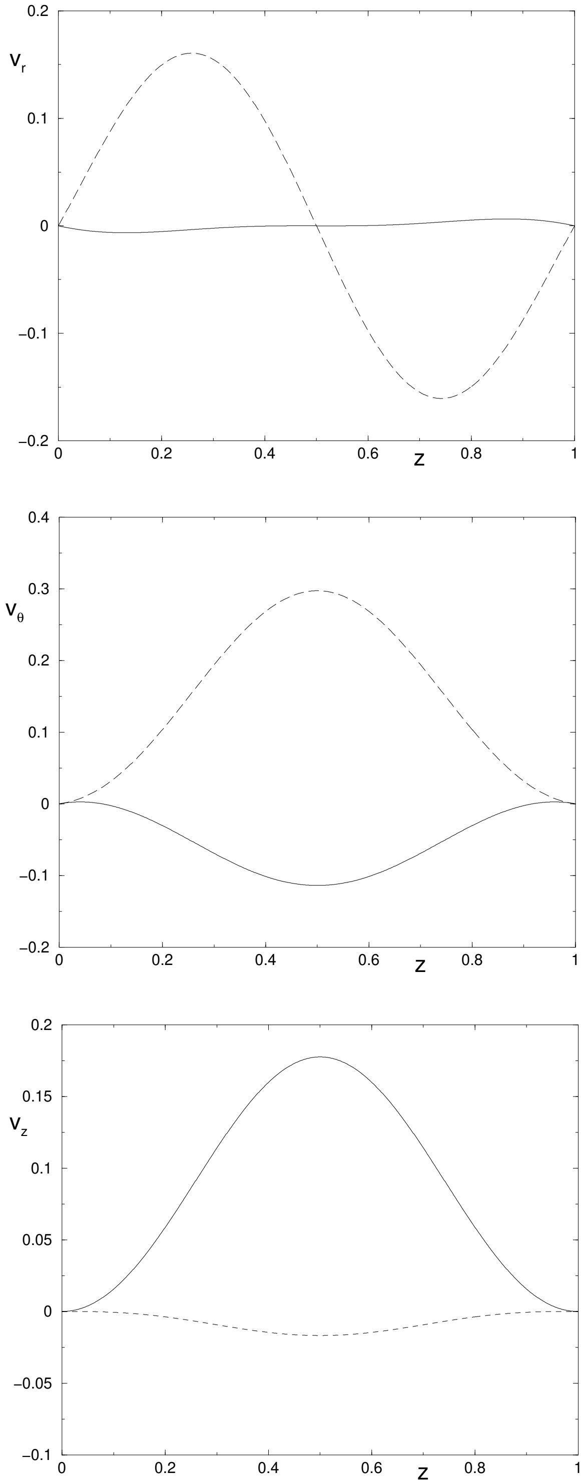

Figure 4.2: The components of the velocity of the linear mode for $De = 3.0$, $R = 2.3$, $\beta = 0.59$ and $\alpha = 3.5$.

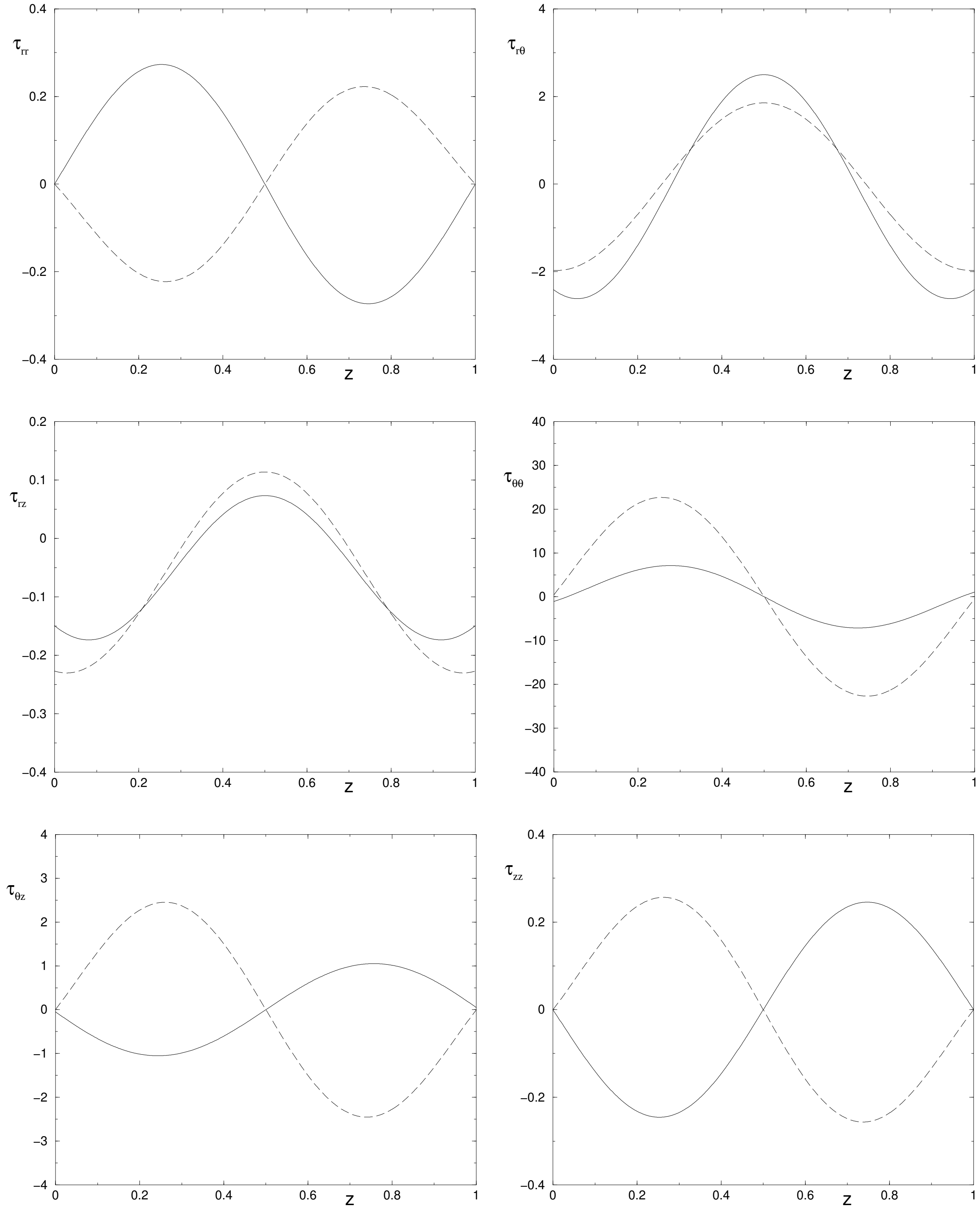

Figure 4.3: The components of the polymeric stress of the linear mode for $De = 3.0$, $R = 2.3$, $\beta = 0.59$ and $\alpha = 3.5$.

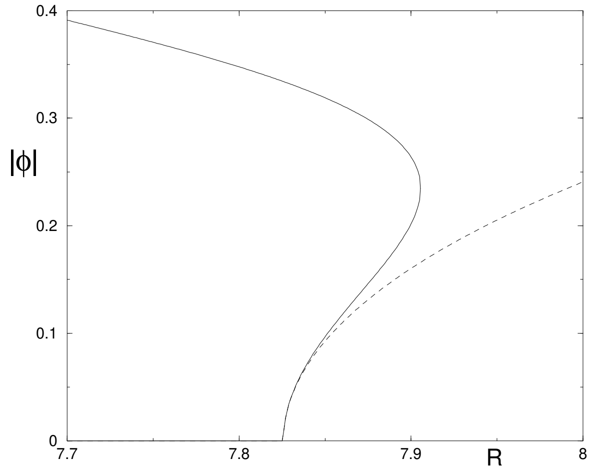

Figure 4.4: The supercritical profile of the first eigenvalue of $De = 2.0$, $\beta = 0.59$ and $\alpha = 6.0$.

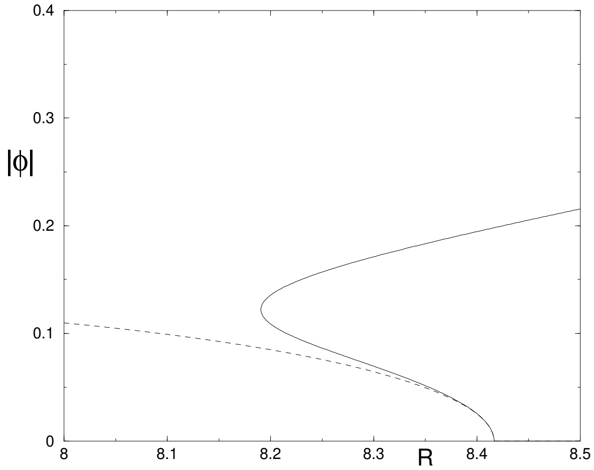

Figure 4.5: The subcritical profile of the second eigenvalue of $De = 2.0$, $\beta = 0.59$ and $\alpha = 6.0$

De	R_c^{sup}	α_c^{sup}	R_c^{sub}	α_c^{sub}
2.0	5.322	2.82	5.456	3.40
3.0	2.106	2.40	2.473	3.88
4.0	1.661	3.81	1.444	4.00

Table 4.2: The smallest combinations of R and α for which we find supercritical and subcritical instabilities. The values for $De = 4.0$ are for the 'second' eigenvalue, because the first is always supercritically unstable.

All the plots so far are made in the region where our approximation $\frac{\Delta r}{R} \ll 1$ (where $r = R + \Delta r$) is valid. However, we can also use our program to see what happens at small values of α (and hence in the region where our approximation might break down). It turns out that the instabilities all get supercritical at some point. Furthermore, the values of R_c as a function of α start to behave like a power law, with $R_c \to \infty$ as $\alpha \downarrow 0$. We can find a formula for this power law by taking the limit $R \to \infty$ of the differential equations that give the linear eigenmodes and eigenfuntions. This gives for the eigenfunctions ($\lambda = \varepsilon + i\omega$)

$$\varepsilon = \frac{\sqrt{R\alpha}}{n\pi} - \frac{1}{\mathit{De}} \qquad \omega = \frac{\sqrt{R\alpha}}{n\pi} \tag{4.1}$$

where n is an integer which is 3 for the least stable eigenvalue, 4 for the next, and so on. The behaviour of R_c of the first eigenvalues of $\mathit{De} = 2.0$, $\mathit{De} = 3.0$ and $\mathit{De} = 4.0$ for $\alpha \downarrow 0$ are plotted in figure 4.10 (solid lines), together with the results found from this formula (dashed lines). We see that it holds well in the region where both α and De are small, but breaks down if one of them increases.

4.5 Conclusions

It turns out that the flow of a viscoelastic fluid between rotating parallel plates is indeed subcritically unstable to axisymmetric disturbances, even at Reynolds number zero. This is in line with the experimental observations reported by McKinley et al. in [7] and [2]. The axisymmetric instability has also been found in recent experiments done in the group of R.G. Larson.

Furthermore, as can be seen from figures 4.6, 4.7 and 4.8, it is important to look at different eigenvalues and modes of the linearized problem to get a complete picture, because it is not always the same mode that is most unstable.

In this thesis, we considered only axisymmetric disturbances. However, there is no reason to expect the non-axisymmetric ones to behave in a different way. We therefore expect the flow to be subcritically unstable to them as well. This statement will be checked by computations in the near future.

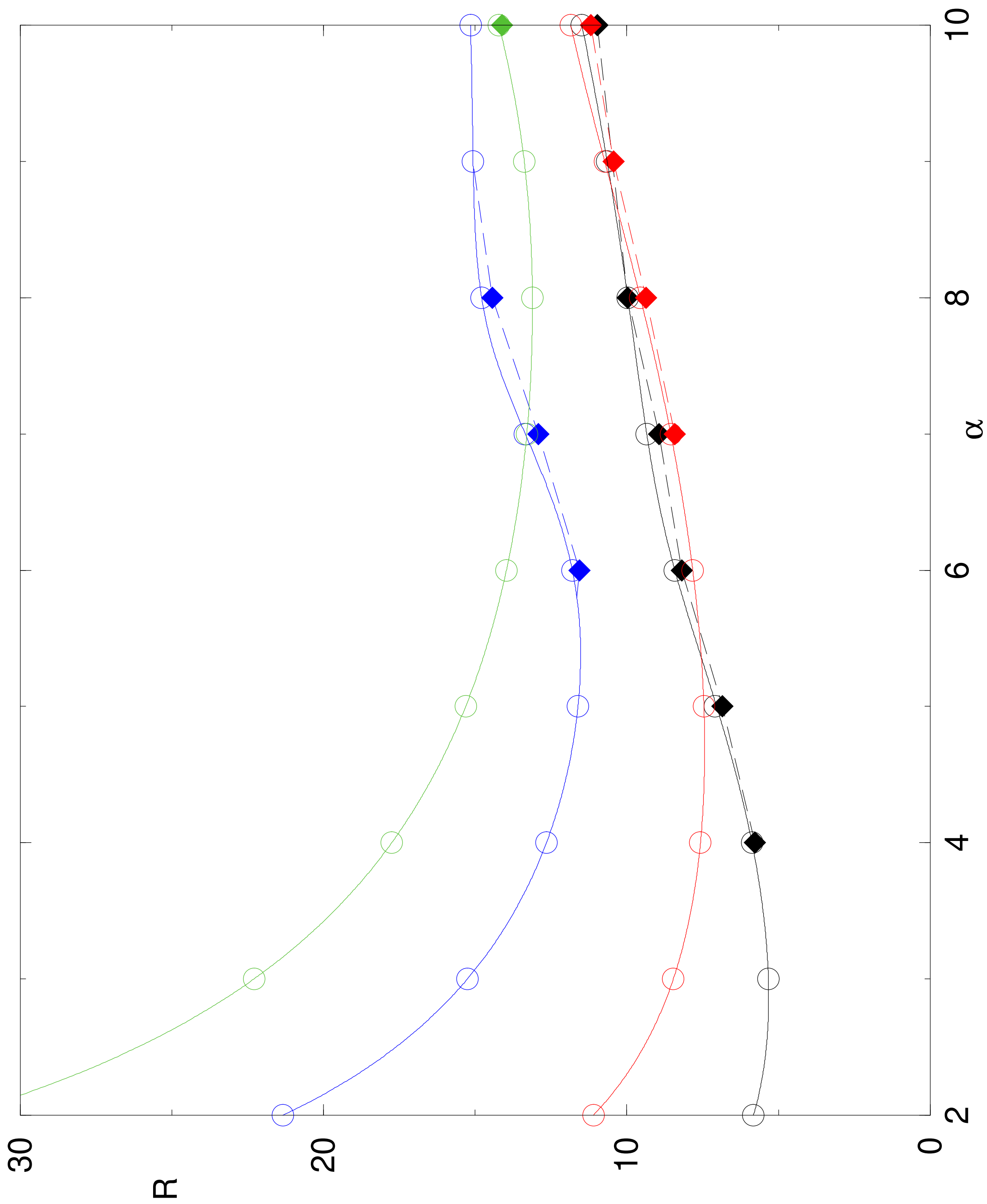

Figure 4.6: R_c and R_s as functions of the wave number α for $De = 2.0$. The open circles represent R_c, the filled diamonds R_s.

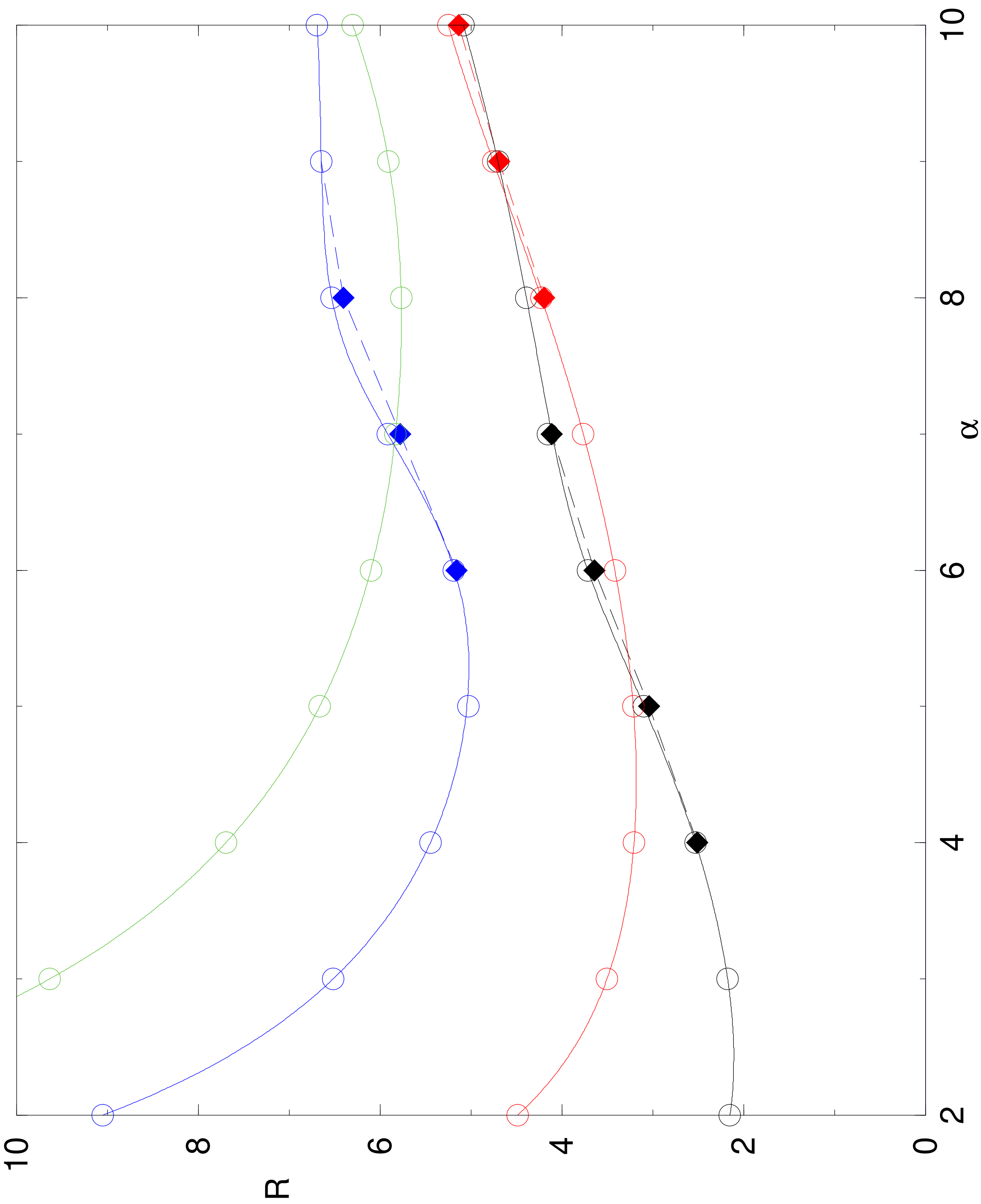

Figure 4.7: R_c and R_s as functions of the wave number α for $De = 3.0$. The open circles represent R_c, the filled diamonds R_s.

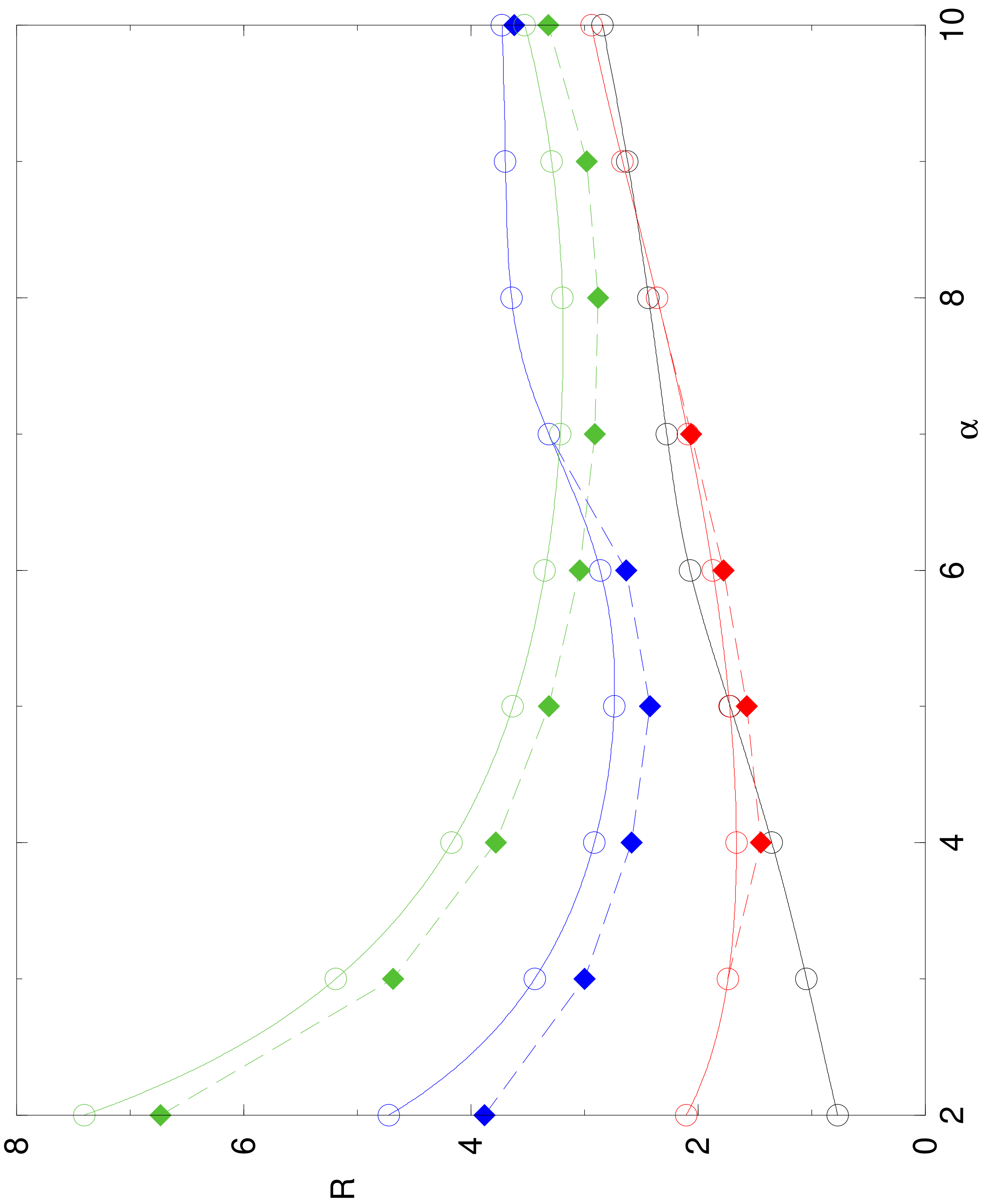

Figure 4.8: R_c and R_s as functions of the wave number α for $De = 4.0$. The open circles represent R_c, the filled diamonds R_s.

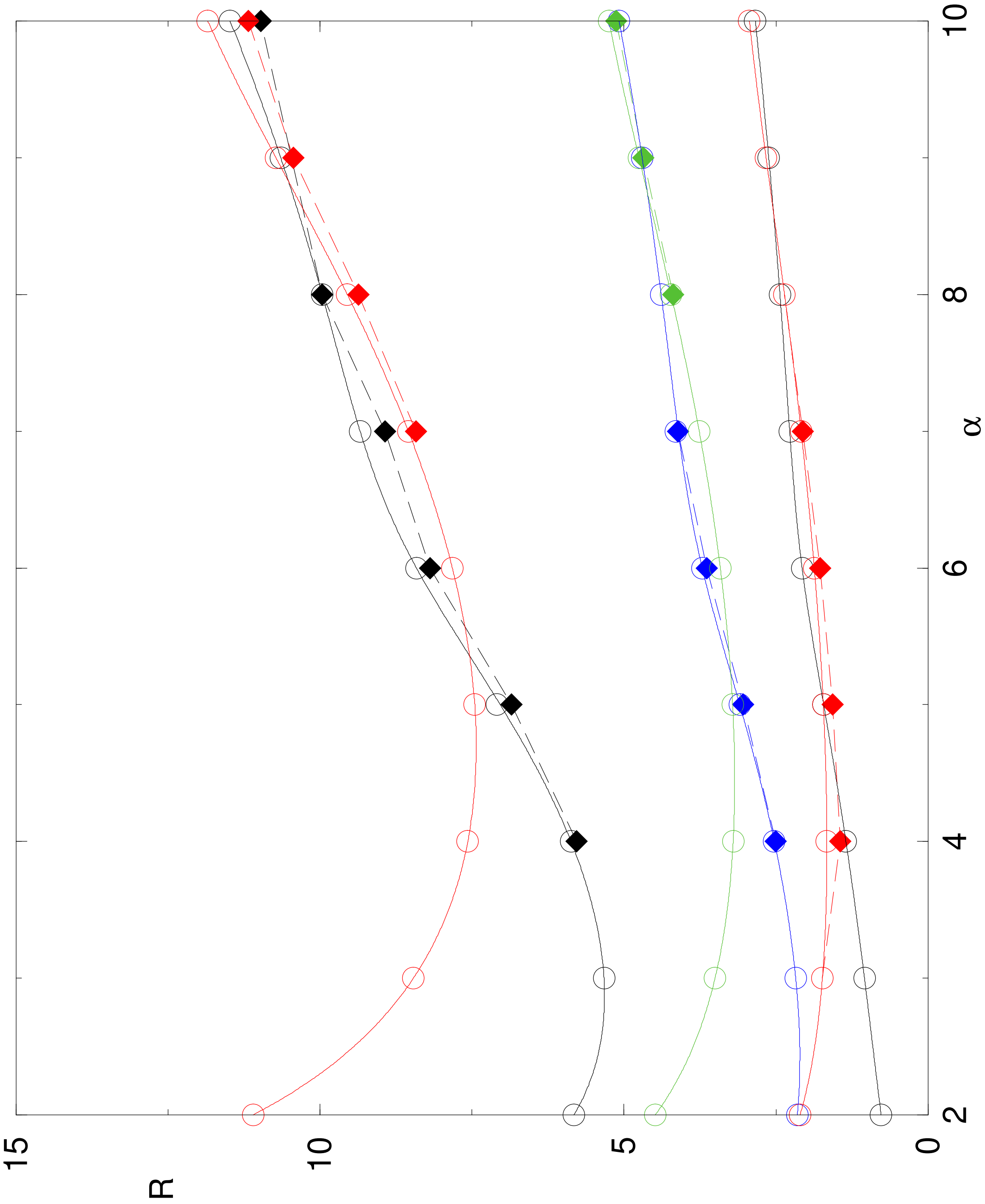

Figure 4.9: R_c and R_s of the first two eigenvalues of (top to bottom) $De = 2.0$, $De = 3.0$ and $De = 4.0$. The open circles represent R_c, the filled diamonds R_s.

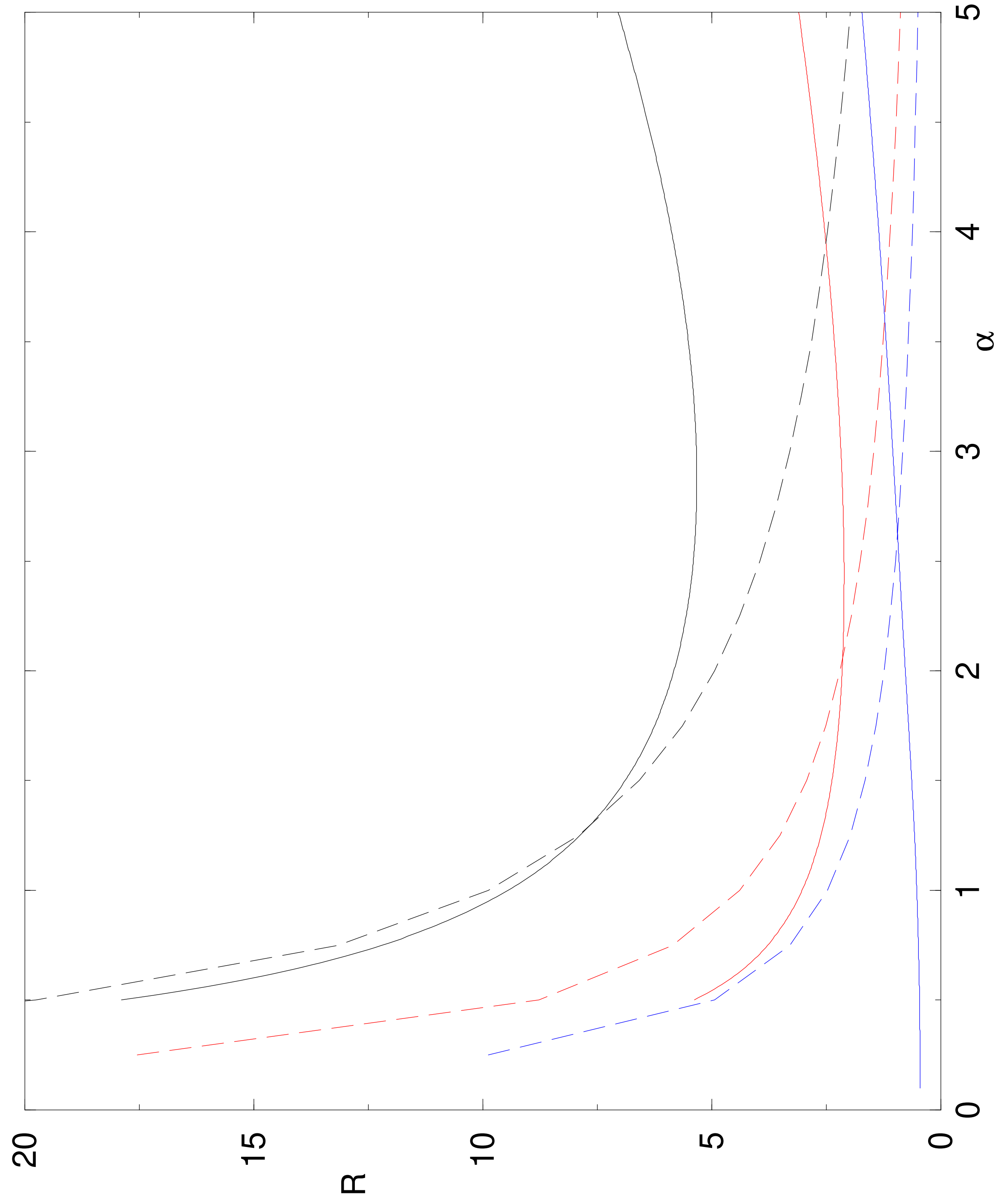

Figure 4.10: Computed and calculated values of R_c in the small-α limit for (top to bottom) $De = 2.0$, $De = 3.0$ and $De = 4.0$

Appendix A

Expressions for the model equations

A.1 The linear operator

From the Oldroyd-B model we got an equation (2.15) of the form

$$\hat{\mathcal{L}}\mathbf{V} + DeA\frac{\partial \mathbf{V}}{\partial t} = N(\mathbf{V}, \mathbf{V}) \tag{A.1}$$

The first four components of this equation are the incompressibility and Navier-Stokes equations. The incompressibility condition ($\vec{\nabla} \cdot \vec{v} = 0$) written out in cylindrical coordinates is given by

$$\vec{\nabla} \cdot \vec{v} = \frac{1}{r}\frac{\partial (r v_r)}{\partial r} + \frac{1}{r}\frac{\partial v_\theta}{\partial \theta} + \frac{\partial v_z}{\partial z} \tag{A.2}$$

For the Navier-Stokes equations (2.5) we have

$$-\vec{\nabla} p - \vec{\nabla} \cdot \overleftrightarrow{\tau} + \beta \Delta \vec{v} = 0 \tag{A.3}$$

or in components

$$\begin{aligned}
0 &= -\frac{\partial p}{\partial r} - \left[\frac{1}{r}\frac{\partial}{\partial r}(r\tau_{rr}) + \frac{1}{r}\frac{\partial}{\partial \theta}\tau_{r\theta} + \frac{\partial}{\partial z}\tau_{rz} - \frac{1}{r}\tau_{\theta\theta}\right] \\
&\quad + \beta\left[\frac{\partial}{\partial r}\left(\frac{1}{r}\frac{\partial}{\partial r}(r v_r)\right) + \frac{1}{r^2}\frac{\partial^2 v_r}{\partial \theta^2} + \frac{\partial^2 v_r}{\partial z^2} - \frac{2}{r^2}\frac{\partial v_\theta}{\partial \theta}\right] && \text{(A.4)} \\
0 &= -\frac{1}{r}\frac{\partial p}{\partial \theta} - \left[\frac{1}{r^2}\frac{\partial}{\partial r}(r^2\tau_{r\theta}) + \frac{1}{r}\frac{\partial}{\partial \theta}\tau_{\theta\theta} + \frac{\partial}{\partial z}\tau_{\theta z}\right] \\
&\quad + \beta\left[\frac{\partial}{\partial r}\left(\frac{1}{r}\frac{\partial}{\partial r}(r v_\theta)\right) + \frac{1}{r^2}\frac{\partial^2 v_\theta}{\partial \theta^2} + \frac{\partial^2 v_\theta}{\partial z^2} + \frac{2}{r^2}\frac{\partial v_r}{\partial \theta}\right] && \text{(A.5)} \\
0 &= -\frac{\partial p}{\partial z} - \left[\frac{1}{r}\frac{\partial}{\partial r}(r\tau_{rz}) + \frac{1}{r}\frac{\partial}{\partial \theta}\tau_{\theta z} + \frac{\partial}{\partial z}\tau_{zz}\right] \\
&\quad + \beta\left[\frac{1}{r}\frac{\partial}{\partial r}\left(r\frac{\partial v_z}{\partial r}\right) + \frac{1}{r^2}\frac{\partial^2 v_z}{\partial \theta^2} + \frac{\partial^2 v_z}{\partial z^2}\right] && \text{(A.6)}
\end{aligned}$$

Defining the operator $L(\cdot) \equiv 1 + De\frac{\partial}{\partial t} + Dez\frac{\partial}{\partial \theta}$, the last six components of equation (2.15) are

$$\begin{aligned}
L(\tau_{rr}) &= -2(1-\beta)\frac{\partial v_r}{\partial r} + N_{rr} && \text{(A.7)}\\
L(\tau_{r\theta}) &= Der\tau_{rz} - 2De^2(1-\beta)r\frac{\partial v_r}{\partial \theta} - De(1-\beta)r\frac{\partial v_r}{\partial z}\\
&\quad -(1-\beta)\left(\frac{\partial v_\theta}{\partial r} + \frac{1}{r}\frac{\partial v_r}{\partial \theta} - \frac{v_\theta}{r}\right) + N_{r\theta} && \text{(A.8)}\\
L(\tau_{rz}) &= -De(1-\beta)\frac{\partial v_r}{\partial \theta} - (1-\beta)\left(\frac{\partial v_z}{\partial r} + \frac{\partial v_r}{\partial z}\right) + N_{rz} && \text{(A.9)}\\
L(\tau_{\theta\theta}) &= 2Der\tau_{\theta z} - 4De^2(1-\beta)r\frac{\partial v_\theta}{\partial \theta} - 2De(1-\beta)r\frac{\partial v_\theta}{\partial z}\\
&\quad -\frac{2}{r}(1-\beta)\left(\frac{\partial v_\theta}{\partial \theta} + v_r\right) + N_{\theta\theta} && \text{(A.10)}\\
L(\tau_{\theta z}) &= Der\tau_{zz} - 2De^2(1-\beta)r\frac{\partial v_z}{\partial \theta} - De(1-\beta)r\frac{\partial v_z}{\partial z} - De(1-\beta)\frac{\partial v_\theta}{\partial \theta}\\
&\quad -(1-\beta)\left(\frac{1}{r}\frac{\partial v_z}{\partial \theta} + \frac{\partial v_\theta}{\partial z}\right) + N_{\theta z} && \text{(A.11)}\\
L(\tau_{zz}) &= -2De(1-\beta)\frac{\partial v_z}{\partial \theta} - 2(1-\beta)\frac{\partial v_z}{\partial z} + N_{zz} && \text{(A.12)}
\end{aligned}$$

Substitution of the Ansatz $\mathbf{V}(r,\theta,z) = e^{i\alpha r}e^{im\theta}e^{i\sigma t}\mathbf{V}(z)$ with $m = 0$ gives the following eigenvalue problem (with $L \equiv 1 - De\sigma$):

$$\begin{aligned}
\frac{\partial^2 v_\theta}{\partial z^2} &= \frac{1}{r^2\left[1+\beta(L-1)\right]}\Big[2 + \beta(L-2) + r\alpha(r\alpha - i)(1+\beta(L-1))\Big]v_\theta(z)\\
&\quad + \frac{De\alpha(r\alpha - 2i)(1-\beta)}{L\left[1+\beta(L-1)\right]}v_z(z) - \frac{Der(iL + r\alpha)(1-\beta)}{L(ra - i)\left[1+\beta(L-1)\right]}\frac{\partial^2 v_z}{\partial z^2}(z) && \text{(A.13)}\\
&\quad \frac{1}{L[1+\beta(L-1)]}\left[\left(\frac{2}{r} + i\alpha\right)\Big(DerN_{rz} + LN_{r\theta}\Big) + L\frac{\partial N_{\theta z}}{\partial z} + Der\frac{\partial N_{zz}}{\partial z}\right]\\
\frac{\partial^4 v_z}{\partial z^4} &= \frac{\alpha^2(1+ir\alpha)^2}{r^2}v_z(z) - \frac{2De(1+L)(1+ir\alpha)(1-\beta)}{Lr\left[1+\beta(L-1)\right]}\frac{\partial^2 v_\theta}{\partial z^2}(z)\\
&\quad + \frac{1}{L^2r^2\left[1+\beta(L-1)\right]}\Big[-2De^2(2+L)r^2(1+ir\alpha)(1-\beta)\\
&\quad + 2L^2(1-\beta)(1 + r\alpha(r\alpha - i)) + \beta L^3(1 + 2r\alpha(r\alpha - i))\Big]\frac{\partial^2 v_z}{\partial z^2} && \text{(A.14)}\\
&\quad + \frac{\left(\frac{1}{r} + i\alpha\right)^2}{1+\beta(L-1)}\left[i\alpha N_{rz} - \frac{\partial N_{rr}}{\partial z}\right]\\
&\quad + \frac{\left(\frac{1}{r} + i\alpha\right)}{1+\beta(L-1)}\left[-\frac{\partial^2 N_{rz}}{\partial z^2} + \frac{1}{r}\frac{\partial N_{\theta\theta}}{\partial z} + \frac{2De}{L}\frac{\partial N_{\theta z}}{\partial z} + \left(\frac{2De^2 r}{L^2} + i\alpha\right)\frac{\partial N_{zz}}{\partial z}\right]
\end{aligned}$$

From (A.13, A.14) we find the equations for the linear mode by taking the nonlinear contributions (the N_{ij}'s) to be zero.

A.2 The adjoint operator

The adjoint operator $\mathcal{L}^+$ of $\mathcal{L}$ is defined in (2.23) by

$$\langle \mathbf{U}, \mathcal{L}\mathbf{V}\rangle = \left\langle \mathcal{L}^+\mathbf{U}, \mathbf{V}\right\rangle \tag{A.15}$$

where

$$\langle \mathbf{U}, \mathbf{V}\rangle \equiv \left(\frac{\alpha}{2\pi}\right)\int_0^{\frac{2\pi}{\alpha}} dr \left(\frac{1}{2\pi}\right)\int_0^{2\pi} d\theta \int_0^1 dz\,(\mathbf{U}, \mathbf{V}) \tag{A.16}$$

We can determine the action of $\mathcal{L}^+$ on $\mathbf{U}$ by partial integration of (A.15). Because integration is a linear operator, we can look at each component of $\mathbf{V}$ separately. This yields the following ten equations, giving a system for the adjoint eigenmodes.

$$\begin{aligned}0 \;=\;& V_1\Bigg\{\frac{1}{r}U_1 - \frac{\partial U_1}{\partial r} + \beta\left[-\frac{1}{r}\frac{\partial U_2}{\partial r} + \frac{\partial^2 U_2}{\partial r^2} + \frac{1}{r^2}\frac{\partial^2 U_2}{\partial \theta^2} + \frac{\partial^2 U_2}{\partial z^2}\right] \\ & -\frac{2\beta}{r^2}\frac{\partial U_3}{\partial \theta} - 2(1-\beta)\frac{\partial U_5}{\partial r} - (2De^2 r + \frac{1}{r})(1-\beta)\frac{\partial U_6}{\partial \theta} \\ & -Der(1-\beta)\frac{\partial U_6}{\partial z} - De(1-\beta)\frac{\partial U_7}{\partial \theta} - (1-\beta)\frac{\partial U_7}{\partial z} + 2\frac{(1-\beta)}{r}U_8\Bigg\}\end{aligned} \tag{A.17}$$

$$\begin{aligned}0 \;=\;& V_2\Bigg\{-\frac{1}{r}\frac{\partial U_1}{\partial \theta} + \frac{2\beta}{r^2}\frac{\partial U_2}{\partial \theta} + \beta\left[-\frac{1}{r}\frac{\partial U_3}{\partial r} + \frac{\partial^2 U_3}{\partial r^2} + \frac{1}{r^2}\frac{\partial^2 U_3}{\partial \theta^2} + \frac{\partial^2 U_3}{\partial z^2}\right] \\ & -(1-\beta)\left(\frac{\partial U_6}{\partial r} + \frac{1}{r}U_6\right) - 2(1-\beta)\left(2De^2 r + \frac{1}{r}\right)\frac{\partial U_8}{\partial \theta} \\ & -2De(1-\beta)r\frac{\partial U_8}{\partial z} - De(1-\beta)\frac{\partial U_9}{\partial \theta} - (1-\beta)\frac{\partial U_9}{\partial z}\Bigg\}\end{aligned} \tag{A.18}$$

$$\begin{aligned}0 \;=\;& V_3\Bigg\{-\frac{\partial U_1}{\partial z} + \beta\left[\frac{1}{r^2}U_4 - \frac{1}{r}\frac{\partial U_4}{\partial r} + \frac{\partial^2 U_4}{\partial r^2} + \frac{1}{r^2}\frac{\partial^2 U_4}{\partial \theta^2} + \frac{\partial^2 U_4}{\partial z^2}\right] \\ & (1-\beta)\frac{\partial U_7}{\partial r} - (1-\beta)\left(2De^2 r + \frac{1}{r}\right)\frac{\partial U_9}{\partial \theta} - De(1-\beta)r\frac{\partial U_9}{\partial z} \\ & -2De(1-\beta)\frac{\partial U_{10}}{\partial \theta} - 2(1-\beta)\frac{\partial U_{10}}{\partial z}\Bigg\}\end{aligned} \tag{A.19}$$

$$0 = V_4\left\{\frac{\partial U_2}{\partial r} + \frac{1}{r}\frac{\partial U_3}{\partial \theta} + \frac{\partial U_4}{\partial z}\right\} \tag{A.20}$$

$$0 = V_5\left\{K(U_5) - \frac{1}{r}U_2 + \frac{\partial U_2}{\partial r}\right\} \tag{A.21}$$

$$0 = V_6\left\{K(U_6) + \frac{1}{r}\frac{\partial U_2}{\partial \theta} + \frac{\partial U_3}{\partial r} - \frac{2}{r}U_3\right\} \tag{A.22}$$

$$0 = V_7\left\{K(U_7) + \frac{1}{r}\frac{\partial U_2}{\partial z} + \frac{\partial U_4}{\partial r} - \frac{1}{r}U_4 - DerU_6\right\} \tag{A.23}$$

$$0 = V_8\left\{K(U_8) + \frac{1}{r}U_2 + \frac{1}{r}\frac{\partial U_3}{\partial \theta}\right\} \tag{A.24}$$

$$0 = V_9\left\{K(U_9) + \frac{\partial U_3}{\partial z} + \frac{1}{r}\frac{\partial U_4}{\partial \theta} - 2DerU_8\right\} \tag{A.25}$$

$$0 = V_{10}\left\{K(U_{10}) + \frac{\partial U_4}{\partial z} - DerU_9\right\} \tag{A.26}$$

where the operator $K(\cdot)$ is defined as

$$K(\cdot) \equiv 1 + De\frac{\partial}{\partial t} + Dez\frac{\partial}{\partial \theta}$$

If we now substitute the Ansatz

$$\mathbf{U}(r,\theta,z,t) = e^{-i\alpha r}e^{-im\theta}e^{\sigma t}\mathbf{U}(z)$$

we get for the axisymmetric modes ($m = 0$) a system of two coupled differential equations:

$$\begin{aligned}
\frac{\partial^2 U_3}{\partial z^2} &= \frac{(1-\beta)}{1+\beta(K-1)}\Bigg\{\left[-i\alpha\frac{K\beta}{1-\beta}\left(\frac{1}{r}+i\alpha\right)+\left(\frac{1}{r}-i\alpha\right)\left(\frac{2}{r}+i\alpha\right)\right]U_3 \\
&\qquad \frac{2iDe}{\alpha}\left(1+K^{-1}\right)\frac{\partial^2 U_4}{\partial z^2}\Bigg\} \qquad (A.27) \\
\frac{\partial^4 U_4}{\partial z^4} &= \frac{-i\alpha(1-\beta)\left(\frac{1}{r}+i\alpha\right)}{1+\beta(K-1)}\Bigg\{i\alpha DerK^{-1}\left(\frac{2}{r}+i\alpha\right)U_3 \\
&\quad +\left[i\alpha\left(\frac{1}{r}+i\alpha\right)+\frac{K\beta}{1-\beta}\left(\frac{1}{r^2}+\frac{i\alpha}{r}-\alpha^2\right)\right]U_4 \qquad (A.28) \\
&\quad +Der\left[1+2K^{-1}-\left(\frac{2}{r}+i\alpha\right)\left(1+K^{-1}\right)\left(\frac{1}{r}+i\alpha\right)^{-1}\right]\frac{\partial^2 U_3}{\partial z^2} \\
&\quad +2\left[1+\frac{K\beta}{1-\beta}+\frac{i}{\alpha r^2}\left(\frac{1}{r}+i\alpha\right)^{-1}-\frac{iDe^2 r}{\alpha K}\left(1+2K^{-1}\right)\right]\frac{\partial^2 U_4}{\partial z^2}\Bigg\}
\end{aligned}$$

where

$$K \equiv 1 - De\sigma$$

A.3 Equations for the $\alpha = 0$ case

Using equations (A.13) and (A.14), we can calculate the linear mode. They can also be used for most of the nonlinear modes (of the form $u_a^{(b)}$), by simply adapting the values of σ and α to that of the mode we are looking for. For the $\alpha = 0$-modes however, these equations are no longer valid, and we need to find the equations for this mode from scratch, meaning that we start with the basic equations (2.4), (2.5) and (2.15), take $m = 0$ and $\alpha = 0$ and extract a set of differential equations like we did before.

This approach yields the following coupled differential equations:

$$
\begin{aligned}
\frac{\partial^2 v_r}{\partial z^2} \quad = \quad & \frac{1}{1+\beta(L-1)}\left\{\frac{1}{r^2}\left[2+\beta(L-2)\right]v_r + 2De(1-\beta)\left(1+\frac{1}{L}\right)\frac{\partial v_\theta}{\partial z}\right. \\
& -\frac{2De^2 r}{L}(1-\beta)\left(1+\frac{2}{L}\right)\frac{\partial v_z}{\partial z} \\
& \left.-\frac{1}{r}\left[\frac{2De^2r^2}{L^2}N_{zz} + \frac{2Der}{L}N_{\theta z} + N_{\theta\theta} - r\frac{\partial N_{rz}}{\partial z} - N_{rr}\right]\right\}
\end{aligned}
\tag{A.29}
$$

$$
\begin{aligned}
\frac{\partial^2 v_r}{\partial z^2} \quad = \quad & \frac{1}{1+\beta(L-1)}\left\{\frac{1}{r^2}\left[2+\beta(L-2)\right]v_\theta - 2De(1-\beta)\left(1+\frac{1}{L}\right)\frac{\partial v_r}{\partial z}\right. \\
& -Der(1-\beta)\left(1+\frac{2}{L}\right)\frac{\partial^2 v_z}{\partial z^2} \\
& \left.+\left[\frac{Der}{L}\frac{\partial N_{zz}}{\partial z} + \frac{\partial N_{\theta z}}{\partial z} + \frac{2De}{L}N_{rz} + \frac{2}{r}N_{r\theta}\right]\right\}
\end{aligned}
\tag{A.30}
$$

A.4 Nonlinear terms

The nonlinear part $N(\mathbf{V},\mathbf{V})$ of (2.15) is given by

$$N(\mathbf{V},\mathbf{V}) = -De\left[\vec{v}\cdot\vec{\nabla}\tau - \left(\vec{\nabla}\vec{v}\right)^{\dagger}\cdot\tau - \tau\cdot\left(\vec{\nabla}\vec{v}\right)\right] \tag{A.31}$$

or, written out in components:

$$N_{rr} = -De(\vec{v}\cdot\vec{\nabla})\tau_{rr} + 2De\left[\tau_{rr}\frac{\partial v_r}{\partial r} + \frac{1}{r}\tau_{r\theta}\frac{\partial v_r}{\partial \theta} + \tau_{rz}\frac{\partial v_r}{\partial z}\right] \tag{A.32}$$

$$\begin{aligned} N_{r\theta} = {} & -De(\vec{v}\cdot\vec{\nabla})\tau_{r\theta} + De\left[\tau_{rr}\left(\frac{\partial v_\theta}{\partial r} - \frac{v_\theta}{r}\right)\right. \\ & \left. +\tau_{r\theta}\left(\frac{\partial v_r}{\partial r} + \frac{v_r}{r} + \frac{1}{r}\frac{\partial v_\theta}{\partial \theta}\right) + \tau_{rz}\frac{\partial v_\theta}{\partial z} + \frac{1}{r}\tau_{\theta\theta}\frac{\partial v_r}{\partial \theta} + \tau_{\theta z}\frac{\partial v_r}{\partial z}\right] \end{aligned} \tag{A.33}$$

$$\begin{aligned} N_{rz} = {} & -De(\vec{v}\cdot\vec{\nabla})\tau_{rz} + De\left[\tau_{rr}\frac{\partial v_z}{\partial r} + \frac{1}{r}\tau_{r\theta}\frac{\partial v_z}{\partial \theta}\right. \\ & \left. +\tau_{rz}\left(\frac{\partial v_z}{\partial z} + \frac{\partial v_r}{\partial r}\right) + \frac{1}{r}\tau_{\theta z}\frac{\partial v_r}{\partial \theta} + \tau_{zz}\frac{\partial v_r}{\partial z}\right] \end{aligned} \tag{A.34}$$

$$\begin{aligned} N_{\theta\theta} = {} & -De(\vec{v}\cdot\vec{\nabla})\tau_{\theta\theta} + 2De\left[\tau_{r\theta}\left(\frac{\partial v_\theta}{\partial r} - \frac{v_\theta}{r}\right)\right. \\ & \left. +\tau_{\theta\theta}\left(\frac{1}{r}\frac{\partial v_\theta}{\partial \theta} + \frac{v_r}{r}\right) + \tau_{\theta z}\frac{\partial v_\theta}{\partial z}\right] \end{aligned} \tag{A.35}$$

$$\begin{aligned} N_{\theta z} = {} & -De(\vec{v}\cdot\vec{\nabla})\tau_{\theta z} + De\left[\tau_{r\theta}\frac{\partial v_z}{\partial r} + \tau_{rz}\left(\frac{\partial v_\theta}{\partial r} - \frac{v_\theta}{r}\right)\right. \\ & \left. +\frac{1}{r}\tau_{\theta\theta}\frac{\partial v_z}{\partial \theta} + \tau_{\theta z}\left(\frac{1}{r}\frac{\partial v_\theta}{\partial \theta} + \frac{v_r}{r} + \frac{\partial v_z}{\partial z}\right) + \tau_{zz}\frac{\partial v_\theta}{\partial z}\right] \end{aligned} \tag{A.36}$$

$$N_{zz} = -De(\vec{v}\cdot\vec{\nabla})\tau_{zz} + 2De\left[\tau_{rz}\frac{\partial v_z}{\partial r} + \frac{1}{r}\tau_{\theta z}\frac{\partial v_z}{\partial \theta} + \tau_{zz}\frac{\partial v_z}{\partial z}\right] \tag{A.37}$$

where $(\vec{v}\cdot\vec{\nabla}) = v_r\frac{\partial}{\partial r} + \frac{v_\theta}{r}\frac{\partial}{\partial \theta} + v_z\frac{\partial}{\partial z}$.

It turns out that we only need a 'symmetrized' version of the general nonlinear functions $N(\mathbf{U},\mathbf{V})$. This means that in all cases that we find them, we either have $\mathbf{U} = \mathbf{V}$ or we encounter N in the symmetrized form

$$[N(\mathbf{U},\mathbf{V})+ \rightleftarrows] \equiv [N(\mathbf{U},\mathbf{V}) + N(\mathbf{V},\mathbf{U})] \tag{A.38}$$

From (A.31) we now have

$$\begin{aligned}
[N(\mathbf{U},\mathbf{V})+ \rightleftarrows] &= -De\Big[\vec{v}\cdot\vec{\nabla}\tau_u - \left(\vec{\nabla}\vec{v}\right)^{\dagger}\cdot\tau_u - \tau_v\cdot\left(\vec{\nabla}\vec{u}\right) \\
&\qquad +\vec{u}\cdot\vec{\nabla}\tau_v - \left(\vec{\nabla}\vec{u}\right)^{\dagger}\cdot\tau_v - \tau_u\cdot\left(\vec{\nabla}\vec{v}\right)\Big] \qquad (A.39)\\
&= -De\Big[\vec{v}\cdot\vec{\nabla}\tau_u - \left(\vec{\nabla}\vec{v}\right)^{\dagger}\cdot\tau_u - \tau_u\cdot\left(\vec{\nabla}\vec{v}\right) \\
&\qquad +\vec{u}\cdot\vec{\nabla}\tau_v - \left(\vec{\nabla}\vec{u}\right)^{\dagger}\cdot\tau_v - \tau_v\cdot\left(\vec{\nabla}\vec{u}\right)\Big] \qquad (A.40)
\end{aligned}$$

so it turns out to be sufficient to write down a function in which we take the vector part from one (say $\mathbf{V}$) and the tensor part from the other (say $\mathbf{U}$) contribution to the symmetric nonlinear function N. From this version we get both $N(\mathbf{V},\mathbf{V})$ and $[N(\mathbf{U},\mathbf{V})+ \rightleftarrows]$.

To avoid confusion, we write

$$\mathbf{V} = e^{i\alpha r}\mathbf{V}(z) \qquad \mathbf{U} = e^{i\gamma r}\mathbf{U}(z)$$

for which we find the following explicit form for the 'first half' of the right-hand side of (A.40):

$$\begin{aligned}
N_{rr} &= iDe(2\alpha-\gamma)\tau_{rr}v_r + 2De\tau_{rz}\frac{\partial v_r}{\partial z} - De\frac{\partial \tau_{rr}}{\partial z}v_z \qquad (A.41)\\
N_{r\theta} &= De(i\alpha - i\gamma + \frac{1}{r})\tau_{r\theta}v_r + De\tau_{\theta z}\frac{\partial v_r}{\partial z} + De\left(i\alpha - \frac{1}{r}\right)\tau_{rr}v_\theta \\
&\quad + De\tau_{rz}\frac{\partial v_\theta}{\partial z} - De\frac{\partial \tau_{r\theta}}{\partial z}v_z \qquad (A.42)\\
N_{rz} &= iDe(\alpha-\gamma)\tau_{rz}v_r + De\tau_{zz}\frac{\partial v_r}{\partial z} + i\alpha De\tau_{rr}v_z - De\frac{\partial \tau_{rz}}{\partial z}v_z + De\tau_{zz}\frac{\partial v_z}{\partial z} \qquad (A.43)\\
N_{\theta\theta} &= De\left(\frac{2}{r} - i\gamma\right)\tau_{\theta\theta}v_r + 2De\left(i\alpha - \frac{1}{r}\right)\tau_{r\theta}v_\theta + 2De\tau_{\theta z}\frac{\partial v_\theta}{\partial z} - De\frac{\partial \tau_{\theta\theta}}{\partial z}v_z \qquad (A.44)\\
N_{\theta z} &= De\left(\frac{1}{r} - i\gamma\right)\tau_{\theta z}v_r + De\left(i\alpha - \frac{1}{r}\right)\tau_{rz}v_\theta + De\tau_{zz}\frac{\partial v_\theta}{\partial z} \\
&\quad + iDe\alpha\tau_{r\theta}v_z - De\frac{\partial \tau_{\theta z}}{\partial z}v_z + De\tau_{\theta z}\frac{\partial v_z}{\partial z} \qquad (A.45)\\
N_{zz} &= -iDe\gamma\tau_{zz}v_r + 2iDe\alpha\tau_{rz}v_z - De\frac{\partial \tau_{zz}}{\partial z}v_z + 2De\tau_{zz}\frac{\partial v_z}{\partial z} \qquad (A.46)
\end{aligned}$$

Appendix B

Expressions for the amplitude equation

For the nonlinear equation (2.15)

$$\hat{\mathcal{L}}\mathbf{V} + A\frac{\partial \mathbf{V}}{\partial t} = N(\mathbf{V},\mathbf{V}), \tag{B.1}$$

we try the Ansatz (2.19):

$$\mathbf{V}(\vec{r},t) = \phi(t)e^{i\alpha r}u_0(z) + \phi^*(t)e^{-i\alpha r}u_0^*(z) + U_{\text{slaved}}. \tag{B.2}$$

Substitution yields an equation for the amplitude ϕ:

$$\begin{aligned}
\hat{\mathcal{L}}\mathbf{V} + A\frac{\partial \mathbf{V}}{\partial t} &= \left[A\frac{\partial \phi}{\partial t} + \lambda\phi\right]e^{i\alpha r}u_0 + \left[A\frac{\partial \phi^*}{\partial t} + \lambda\phi^*\right]e^{-i\alpha r}u_0^* + A\frac{\partial U_{\text{slaved}}}{\partial t} + \hat{\mathcal{L}}U_{\text{slaved}} \\
&= \phi^2 N(e^{i\alpha r}u_0, e^{i\alpha r}u_0) + c.c. + |\phi|^2\left[N(e^{i\alpha r}u_0, e^{-i\alpha r}u_0^*) + \rightleftarrows\right] \qquad \text{(B.3)} \\
&+ \quad \phi\left[N(e^{i\alpha r}u_0, U_{\text{slaved}}) + \rightleftarrows\right] + \phi^*\left[N(e^{-i\alpha r}u_0^*, U_{\text{slaved}}) + \rightleftarrows\right] \\
&+ \quad N(U_{\text{slaved}}, U_{\text{slaved}}),
\end{aligned}$$

where $\rightleftarrows$ again means that we take the previous term with the arguments switched (so $N(A,B)+\rightleftarrows$ stands for $N(A,B)+N(B,A)$).

Using the inner product (2.22)

$$\langle \mathbf{U},\mathbf{V}\rangle \equiv \left(\frac{\alpha}{2\pi}\right)\int_0^{\frac{2\pi}{\alpha}} dr \left(\frac{1}{2\pi}\right)\int_0^{2\pi} d\theta \int_0^1 dz\,(\mathbf{U},\mathbf{V}), \tag{B.4}$$

we can select a single 'Fourier mode' from (B.3). Taking that to be the $e^{i\alpha r}$-mode we find an equation for ϕ:

$$\begin{aligned}
\left[A\frac{\partial \phi}{\partial t} + \lambda\phi\right]e^{i\alpha r}u_0 &= \phi\left[N(e^{i\alpha r}u_0, U_{\text{slaved}}) + \rightleftarrows\right] + \phi^*\left[N(e^{-i\alpha r}u_0^*, U_{\text{slaved}}) + \rightleftarrows\right] \\
&\quad + \sum_{n=2}^{\infty}\left[N(V_{n+1}e^{in\alpha r}e^{i\alpha r}, V_n^* e^{-in\alpha r}) + \rightleftarrows\right], \qquad \text{(B.5)}
\end{aligned}$$

where the first two terms of the right-hand side of (B.5) are of order ϕ^3, whereas the smallest-order contribution of the third terms is $\mathcal{O}(\phi^5)$.

Equation (B.5) is an amplitude equation of the general form (2.25)

$$A\frac{\partial\phi}{\partial t} = C_1\phi + C_3\phi|\phi|^2 + C_5\phi|\phi|^4 + \dots \tag{B.6}$$

To first order in ϕ we find from (B.5)

$$A\frac{\partial\phi}{\partial t} = -\lambda\phi, \tag{B.7}$$

so $C_1 = -\lambda$.

Going to third order in ϕ, (B.5) gives:

$$\left[A\frac{\partial\phi}{\partial t} + \lambda\phi\right]\langle\bar{m}(z)|u_0(z)\rangle = \phi|\phi|^2\left\langle e^{-i\alpha r}\bar{m}(z)|N(e^{i\alpha r}u_0, u_0^{(2)}) + \rightleftarrows + N(e^{-i\alpha r}u_0^*, e^{2i\alpha r}u_2^{(2)}) + \rightleftarrows\right\rangle, \tag{B.8}$$

so C_3 is given by

$$C_3 = \frac{\left\langle e^{-i\alpha r}\bar{m}(z)|N(e^{i\alpha r}u_0, u_0^{(2)}) + \rightleftarrows + N(e^{-i\alpha r}u_0^*, e^{2i\alpha r}u_2^{(2)}) + \rightleftarrows\right\rangle}{\langle\bar{m}(z)|u_0(z)\rangle}. \tag{B.9}$$

To compute C_3 from this expression, we first need to find the functions $u_2^{(2)}$ and $u_0^{(2)}$. To do that, we look at the $e^{2i\alpha r}$ and $e^{0i\alpha r}$ modes respectively. They give the following equations for these functions:

$$\hat{\mathcal{L}}\left(e^{2i\alpha r}u_2^{(2)}\right) - 2\lambda e^{2i\alpha r}u_2^{(2)} = N\left(e^{i\alpha r}u_0, e^{i\alpha r}u_0\right) \tag{B.10}$$

$$\hat{\mathcal{L}}\left(u_0^{(2)}\right) - (\lambda + \lambda^*)u_0^{(2)} = N\left(e^{i\alpha r}u_0, e^{-i\alpha r}u_0^*\right) + \rightleftarrows \tag{B.11}$$

Finally, going to fifth order in ϕ, we find the expression for C_5:

$$C_5 = \frac{\left\langle e^{-i\alpha r}\bar{m}(z)|N(e^{i\alpha r}u_0, u_0^{(4)}) + \rightleftarrows + N(e^{-i\alpha r}u_0^*, e^{2i\alpha r}u_2^{(4)}) + \rightleftarrows + N(e^{3i\alpha r}u_3^{(3)}, e^{-2i\alpha r}u_2^{(2)^*}) + \rightleftarrows\right\rangle}{\langle\bar{m}(z)|u_0(z)\rangle}. \tag{B.12}$$

Where we find $u_3^{(3)}$, $u_2^{(4)}$ and $u_0^{(4)}$ from the $e^{3i\alpha r}$, $e^{2i\alpha r}$ and $e^{0i\alpha r}$ modes:

$$\hat{\mathcal{L}}\left(e^{3i\alpha r}u_3^{(3)}\right) - 3\lambda e^{3i\alpha r}u_3^{(3)} = N(e^{i\alpha r}u_0, e^{2i\alpha r}u_2^{(2)}) + \rightleftarrows \tag{B.13}$$

$$\hat{\mathcal{L}}\left(e^{2i\alpha r}u_2^{(4)}\right) + 2C_3e^{2i\alpha r}u_2^{(2)} - (3\lambda + \lambda^*)e^{2i\alpha r}u_2^{(4)} = \tag{B.14}$$
$$N(e^{2i\alpha r}u_2^{(2)}, u_0^{(2)}) + \rightleftarrows + N(e^{-i\alpha r}u_0^*, e^{3i\alpha r}u_3^{(3)}) + \rightleftarrows$$

$$\hat{\mathcal{L}}\left(u_0^{(4)}\right) + 2\mathrm{Re}(C_3)u_0^{(2)} - 4\mathrm{Re}(\lambda)u_0^{(4)} = N(e^{2i\alpha r}u_2^{(2)}, e^{-2i\alpha r}u_2^{(2)^*}) + \rightleftarrows + N(u_0^{(2)}, u_0^{(2)}) \tag{B.15}$$

Appendix C

Numerical methods and algorithms

In this appendix, we derive the expressions for the components of the projection matrix P in (3.19). We also print the relevant part of the C-code of the algorithms from chapter 3.

C.1 The projection matrix

We are looking for a 3×3 upper-triangular matrix P which projects any $n \times 3$ matrix Y onto a $n \times 3$ matrix Z by post-multiplication:

$$Z = YP \tag{C.1}$$

In general we have

$$Y = \begin{pmatrix} y_1^{(1)} & y_1^{(2)} & y_1^{(3)} \\ y_2^{(1)} & y_2^{(2)} & y_2^{(3)} \\ y_3^{(1)} & y_3^{(2)} & y_3^{(3)} \\ \vdots & \vdots & \vdots \\ y_n^{(1)} & y_n^{(2)} & y_n^{(3)} \end{pmatrix} \qquad Z = \begin{pmatrix} z_1^{(1)} & z_1^{(2)} & z_1^{(3)} \\ z_2^{(1)} & z_2^{(2)} & z_2^{(3)} \\ z_3^{(1)} & z_3^{(2)} & z_3^{(3)} \\ \vdots & \vdots & \vdots \\ z_n^{(1)} & z_n^{(2)} & z_n^{(3)} \end{pmatrix} \tag{C.2}$$

and

$$P = \begin{pmatrix} p_{11} & p_{12} & p_{13} \\ 0 & p_{22} & p_{23} \\ 0 & 0 & p_{33} \end{pmatrix} \tag{C.3}$$

Applying the Gramm-Schmidt process yields the following expressions for the columns $z^{(i)}$ of Z:

$$\begin{aligned} w_{11} &= |y^{(1)}| \\ z^{(1)} &= \frac{y^{(1)}}{w_{11}} \end{aligned} \tag{C.4}$$

$$\begin{aligned} w_{22} &= |y^{(2)} - \left(y^{(2)}, z^{(1)}\right) z^{(1)}| \\ z^{(2)} &= \frac{y^{(2)} - \left(y^{(2)}, z^{(1)}\right) z^{(1)}}{w_{22}} \\ &= \frac{y^{(2)}}{w_{22}} - \frac{y^{(1)} \left(y^{(2)}, z^{(1)}\right)}{w_{11} w_{22}} \end{aligned} \tag{C.5}$$

$$
\begin{aligned}
w_{33} &= |y^{(3)} - \left(y^{(3)}, z^{(1)}\right) z^{(1)} - \left(y^{(3)}, z^{(2)}\right) z^{(2)}| \\
z^{(3)} &= \frac{y^{(3)} - \left(y^{(3)}, z^{(1)}\right) z^{(1)} - \left(y^{(3)}, z^{(2)}\right) z^{(2)}}{w_{33}} \\
&= \frac{y^{(3)}}{w_{33}} - \frac{y^{(1)} \left(y^{(3)}, z^{(1)}\right)}{w_{11} w_{33}} - \frac{y^{(2)} \left(y^{(3)}, z^{(2)}\right)}{w_{22} w_{33}} + \frac{y^{(1)} \left(y^{(2)}, z^{(1)}\right) \left(y^{(3)}, z^{(2)}\right)}{w_{11} w_{22} w_{33}}
\end{aligned} \tag{C.6}
$$

where

$$|y| = (y, y)^{\frac{1}{2}}$$

On the other hand, we have from equation (C.1)

$$z^{(1)} = p_{11} y^{(1)} \tag{C.7}$$

$$z^{(2)} = p_{12} y^{(1)} + p_{22} y^{(2)} \tag{C.8}$$

$$z^{(3)} = p_{13} y^{(1)} + p_{23} y^{(2)} + p_{33} y^{(3)} \tag{C.9}$$

If we now choose

$$p_{11} = \frac{1}{w_{11}} \qquad p_{22} = \frac{1}{w_{22}} \qquad p_{33} = \frac{1}{w_{33}} \tag{C.10}$$

we find from combining (C.4) and (C.7) that indeed

$$z^{(1)} = p_{11} y^{(1)}$$

Combining (C.5) and (C.8) gives

$$
\begin{aligned}
p_{22} &= \frac{1}{w_{22}} \\
p_{12} &= \frac{z^{(2)} - p_{22} y^{(2)}}{y^{(1)}} = \frac{1}{y^{(1)}} \left[\frac{y^{(2)}}{w_{22}} - \frac{y^{(1)} \left(y^{(2)}, z^{(1)}\right)}{w_{11} w_{22}} - \frac{y^{(2)}}{w_{22}} \right] \\
&= -\frac{\left(z^{(1)}, y^{(2)}\right)}{w_{11} w_{22}}
\end{aligned}
$$

and from (C.6) and (C.9) we find

$$
\begin{aligned}
p_{33} &= \frac{1}{w_{33}} \\
p_{23} &= -\frac{\left(z^{(2)}, y^{(3)}\right)}{w_{22} w_{33}} \\
p_{13} &= -\frac{\left(z^{(1)}, y^{(3)}\right)}{w_{11} w_{33}} + \frac{\left(z^{(1)}, y^{(2)}\right) \left(z^{(2)}, y^{(3)}\right)}{w_{11} w_{22} w_{33}}
\end{aligned}
$$

C.2 RK4

```
void rk4(double x, int k, complex double *y, int n, complex double sigma,
double a, complex double **fext, double h, int na, complex double *yout) {
  int i;
  double h2, h6;
  complex double *dydx, *dym, *dyt, *yt, *ftemp;
  /* Perform rk4 on the (n-dim) vector y from starting point x.
   * The (optional) non-linear contribution to the derivatives (which are
   * computed using the 'derivs' function) is given in fext.
   * The variable na indicates whether we are computing a linear or an
   * adjoint mode. The stepsize is h.
   * The final value (in x+h) is returned in yout.
   * In the comments, the differential equation is indicated as
   * dydx = f(x,y).
   */

  dydx = cvector(1,n);
  dym = cvector(1,n);
  dyt = cvector(1,n);
  yt = cvector(1,n);
  ftemp = cvector(1,2);
  h2 = h/2.0;
  h6 = h/6.0;

  /* First step: determine the y-value halfway (necessary to determine k2).
   * We are looking from the previous point (k-1).
   */
  ftemp[0] = fext[k-1][0];
  ftemp[1] = fext[k-1][1];
  derivs(x, y, dydx, sigma, a, ftemp, na);
  for (i=0; i<n; i++) yt[i] = y[i] + h2*dydx[i];

  /* Second step: k2 = dyt = derivs(x+h2,yt,dyt) *
   * Determine the y-value for k3
   */
  ftemp[0] = (fext[k-1][0] + fext[k][0])/2.0;
  ftemp[1] = (fext[k-1][1] + fext[k][1])/2.0;
  derivs(x+h2, yt, dyt, sigma, a, ftemp, na);
  for (i=0; i<n; i++) yt[i] = y[i] + h2*dyt[i];

  /* Third step: k3 = dym = derivs(x+h2, yt, dym). *
   * Determine the y-value for k4; join dym and dyt.
   */
  derivs(x+h2, yt, dym, sigma, a, ftemp, na);
  for (i=0; i<n; i++) {
    yt[i] = y[i] + h*dym[i];
```

```
    dym[i] += dyt[i];
  }

  /* Fourth step: k4 */
  ftemp[0] = fext[k][0];
  ftemp[1] = fext[k][1];
  derivs(x+h, yt, dyt, sigma, a, ftemp, na);
  /* Join all together with proper weighing factors */
  for (i=0; i<n; i++) yout[i] = y[i] + h6*(dydx[i] + 2.0*dym[i] + dyt[i]);

  free_cvector(dydx,1,n);
  free_cvector(yt,1,n);
  free_cvector(dyt,1,n);
  free_cvector(dym,1,n);
  free_cvector(ftemp,1,2);
} /* rk4 */
```

C.3 Shoot

The shooting algorithm consists of three functions: an ode-integrator (`odeint`), a function that performes a single shot (`shootonce`) and a function that checks the results of the shot and adapts the starting values (`shoot`).

```
void odeint(double *x1, double *x2, complex double *y, complex double sigma,
int n, int nsteps) {
  /* Perform rk4 integration from x1 to x2 in nsteps steps */
  int i, k;
  double x, h = (*x2 - *x1) / (double)nsteps;
  complex double *yout, *dy;
  yout = cvector(1,n);
  dy = cvector(1,n);

  x = *x1;
  if (x+h == x) nrerror("Stepsize too small for rk4 integration");

  for (k=1; k<=nsteps; k++) {
    derivs(x, y, dy, sigma);
    rk4(x, y, n, dy, sigma, h, yout);
    x = x+h;
    for (i=0; i<n; i++) y[i] = yout[i];
  }

  free_cvector(yout,1,n);
  free_cvector(dy,1,n);
} /* odeint */
```

```
void shootonce(int N, int n2, double *x1, double *x2, complex double *v,
complex double *y, complex double *deltav, int steps, complex double *F,
complex double *dv, complex double sigma) {
  /* Perform a single cycle of the shooting method.
   * We integrate the N functions from x1 to x2 using rk4.
   * There are n2 boundary conditions that are freely specified.
   * Their initial guess is input in v. The size of the increments
   * used to determine the Jacobian is given in deltav.
   * Steps is the number of steps to be used in RK4.
   *
   * After integration, we have a difference between the required and
   * actual value of the function(s) at x2. Using Newton's method, we
   * get from this an adjustment of the free parameters at x1. The new
   * parameters are returned in v. The alterations are returned in dv
   * and the discrepancy vector is returned in F.
   */

  int i, j;
  int *indx; /* Vector used in LUdecomp */
  complex double det, sav; /* det is used in LUdecomp */
  complex double *dy; /* Vector used in integration */
  complex double **dFdV; /* Jacobian matrix of F at x2 */
  indx = ivector(1,n2);
  dy = cvector(1,N);
  dFdV = cmatrix(1,n2,1,n2);

  /* Get the value of y in x1 */
  load(*x1, v, y);

  /* Integrate from x1 to x2 using the trial values given in *v */
  odeint(x1, x2, y, sigma, N, steps);

  /* Determine the discrepancy vector we get with these trial values */
  Fvec(*x2, y, F);

  /* Perform Newton's method to determine an improvement of v.
   * This means we vary the boundary conditions at x1, integrate to x2,
   * use this result to determine the Jacobian of the discrepancy
   * vector (F) at x2 and finally solve J*dV = -F. (J = dFdV) */

  /* First step: determine Jacobian dFdV */
  for (j=0; j<n2; j++) {
    sav = v[j];
    v[j] += deltav[j]; /* deltav is input */
    load(*x1, v, dy);
    odeint(x1, x2, dy, sigma, N, steps);
```

```
    /* At this point, dv contains the difference we get if we vary just
     * one component of v; we need this information to calculate the
     * Jacobian of F. */
    Fvec(*x2, dy, dv);
    for (i=0; i<n2; i++) {
      dFdV[i][j] = (dv[i] - F[i]) / deltav[j];
    }
    v[j] = sav;
  }

  /* Second step: solve the system J*dv = -F */
  for (i=0; i<n2; i++) dv[i] = -F[i];
  Cramer(n2, dFdV, dv, -F);

  /* Add dv to v to get a better guess for the initial parameters */
  for (i=0; i<n2; i++) v[i] += dv[i];

  free_cvector(dy,1,N);
  free_ivector(indx);
  free_cmatrix(dFdV, 1, n2, 1, n2);
} /* shootonce */


int shoot(int N, int n2, double *x1, double *x2, complex double *y,
complex double *v, complex double sigma) {
  /* Perform the shooting method by repeated calling of shootonce and
   * subsequently checking if the result is good enough yet */
  int j;
  complex double *F, *dV, *deltav;
  F = cvector(1,n2);
  dV = cvector(1,n2);
  deltav = cvector(1,n2);

  for (j=0; j<n2; j++) {
    deltav[j] = 0.01 + I*0.01;
    dV[j] = 0.1 + I*0.1;
  }

  while (maximum(dV, n2) > 0.001) {
    shootonce(N, n2, x1, x2, v, y, deltav, intsteps, F, dV, sigma);
  }

  free_cvector(F,1,n2);
  free_cvector(dV,1,n2);
  free_cvector(deltav,1,n2);
  return j;
} /* shoot */
```

C.4 Godunovforward

```
void godunovforward(double *x1, double *x2, int N, int n2, complex double ***U,
complex double **upart, complex double ***P, complex double **Omega, complex
double sigma, double a, complex double **fext, int na) {
  /* Integrate the equations using the rk4 method; at each mesh point we
   * re-orthonormalize the matrix of homogeneous solution and adapt the
   * particular solution.
   * All intermediate steps are stored, as well as the matrices used for
   * orthonormalization. The value returned is the matrix of repeatedly
   * re-orthonormalized solutions at the endpoint x2. (These are used to
   * reconstruct the 'true' values of the functions elsewhere.)
   * Sigma is the 'eigenvalue', meaning the trial eigenvalue for the linear
   * and adjoint modes, and the combination of eigenvalues used for the
   * nonlinear modes. The value of a is alpha for the linear and adjoint modes
   * and a multiple of alpha for the nonlinear modes.
   * The function fext contains the nonlinear contribution to the equations.
   * The variable na ('normal-adjoint') is 1 if we are calculating the
   * eigenvalue of the 'normal' linear mode, and 2 if we are calculating it for
   * the adjoint mode.
   */

  int i, j, k;
  double x, h;
  complex double **Y; /* Matrix of homogeneous solutions */
  complex double *ypart;   /* Particular solution in case of inhomogeneous
    * system */
  complex double *yout;
  complex double *ytemp;
  complex double **nulvector; /* Vector used as 'external contribution'
    * in case of a linear equation. */

  complex double A,B,L;

  Y = cmatrix(1,N,1,n2);
  ypart = cvector(1,N);
  Yload(Y, ypart, N, n2);

  yout = cvector(1,N);
  ytemp = cvector(1,N);

  nulvector = cmatrix(1,intsteps,1,2);
  for (i=0; i<intsteps; i++) {
    nulvector[i][0] = 0.0;
    nulvector[i][1] = 0.0;
  }
```

```
  x = *x1;
  h = (*x2 - *x1) / (double)(intsteps-1);
  if (x+h == x) nrerror("Stepsize too small for rk4 integration");

  for (i=0; i<N; i++) {
    for (j=0; j<n2; j++) {
      U[0][i][j] = Y[i][j];
    }
    upart[0][i] = ypart[i];
  }

  for (k=1; k<intsteps; k++) {

    /* Perform rk4 'integration' from x to x+h */
    for (i=0; i<n2; i++) {
      for (j=0; j<N; j++) {
        ytemp[j] = Y[j][i];
      }
      rk4(x, k, ytemp, N, sigma, a, nulvector, h, na, yout);
      for (j=0; j<N; j++) Y[j][i] = yout[j];
    }
    rk4(x, k, ypart, N, sigma, a, fext, h, na, yout);
    for (j=0; j<N; j++) ypart[j] = yout[j];
    x=x+h;

    /* Re-orthonormalize */
    orthonormalize(Y, P[k], N, n2);
    orthorescale(ypart, Y, Omega[k], N, n2);

    /* Store the intermediate result in the matrix U(k) and vector upart(k) */
    for (i=0; i<N; i++) {
      for (j=0; j<n2; j++) {
        U[k][i][j] = Y[i][j];
      }
      upart[k][i] = ypart[i];
    }

  }

  free_cmatrix(Y,1,N,1,n2);
  free_cvector(ypart, 1, n2);
  free_cvector(ytemp, 1, N);
  free_cvector(yout, 1, N);
  free_cmatrix(nulvector,1,intsteps,1,2);

} /* godunovforward */
```

C.5 Godunovbackward

```
void godunovbackward(double *x1, double *x2, int N, int n2, complex double ***U,
complex double **upart, complex double ***P, complex double **Omega, complex
double sigma, int eqtype, complex double **Y) {
  /* Reconstruct the eigenfunctions of both the normal and the adjoint mode
   * on the full interval (x1, x2). We start at the endpoint with the solutions
   * obtained in godunov(). With the stored intermediate (U, upart) values and
   * the orthonormalization matrices (P, Omega) we can now re-compute the true
   * value of Y at each mesh point.
   * The parameter eqtype makes the difference between a linear and a nonlinear
   * equation (matters for betafinal).
   * Instead of storing the values of Y in a file, we now return them to be
   * used in another calculation.
   */

  int i,j,k;
  double x, h;
  complex double *betavector, *tempvector;

  betavector = cvector(1,n2);
  tempvector = cvector(1,n2);

  /* Determine the solution vector at the endpoint */
  betafinal(betavector, U[intsteps-1], upart[intsteps-1], n2, eqtype);
  for (i=0; i<N; i++) {
    Y[intsteps-1][i] =  upart[intsteps-1][i];
    for (j=0; j<n2; j++) {
      Y[intsteps-1][i] += betavector[j]*U[intsteps-1][i][j];
    }
  }

  /* Sweep backward */
  for (k=intsteps-2; k>=0; k--) {
    /* Compute new betavector: beta = P*(betaold-omega) */
    for (i=0; i<n2; i++) {
       tempvector[i] = betavector[i] - Omega[k+1][i];
    }
    matrixvectorproduct(P[k+1],tempvector,betavector,n2,n2);

    /* Compute Y */
    for (i=0; i<N; i++) {
      Y[k][i] =  upart[k][i];
      for (j=0; j<n2; j++) {
        Y[k][i] += betavector[j]*U[k][i][j];
      }
    }
```

```
  }

  free_cvector(betavector,1,n2);
  free_cvector(tempvector,1,n2);

} /* godunovbackward */
```

Bibliography

[1] R.B. Bird, R.C. Armstrong, and O. Hassager, *Dynamics of polymeric liquids - volume 1: Fluid mechanics*, 2nd ed., John Wiley & Sons, New York, 1987.

[2] J.A. Byars, A. Öztekin, R.A. Brown, and G.H. McKinley, *Spiral instabilities in the flow of highly elastic fluids between rotating parallel disks*, Journal of Fluid Mechanics **271** (1994), 173–218.

[3] S.D. Conte, *The numerical solution of linear boundary value problems*, SIAM Review **8** (1966), 309–321.

[4] A. Groisman and V. Steinberg, *Elastic turbulence in a polymer solution flow*, Nature **405** (2000), 53–55.

[5] L.D. Landau and E.M. Lifshitz, *Fluid mechanics*, 2nd ed., Pergamon, Oxford, 1987.

[6] R.G. Larson, *Turbulence without inertia*, Nature **405** (2000), 27–28.

[7] G.H. McKinley, J.A. Byars, R.A. Brown, and R.C. Armstrong, *Observations on the elastic instability in cone-and-plate and parallel-plate flows of a polyisobutylene boger fluid*, Journal of Non-Newtonian Fluid Mechanics **40** (1991), 201–229.

[8] A. Öztekin and R.A. Brown, *Instability of a viscoelastic fluid between rotating parallel disks: analysis for the Oldroyd-B fluid*, Journal of Fluid Mechanics **255** (1993), 473–502.

[9] W.H. Press, B.P. Flannery, S.A. Teukolsky, and W.T. Vetterling, *Numerical recipes in C*, 1st ed., Cambridge University Press, 1988.

[10] K. Weissenberg, Nature **159** (1947), 310–311.

Acknowledgement

The research, of which the results are given in this thesis, I did in collaboration with Alexander Morozov. His help has been of great value, and, apart from that, I enjoyed working with him on this project.

The work was done in the group and under the supervision of Wim van Saarloos. When he was temporarily unavailable due to illness, Pierre van Baal was kind enough to take over supervision.

Apart from them, there are of course many people who contributed in a way to this thesis and my physics study in general. To list all of these family members, friends, teachers and fellow students would result in a Homeric (and therefore undesirable) long list which would nevertheless always fail to mention someone who would have a right to be on it. However, particularly during the research that lead to this thesis, I spent many long days in the company of four fellow students, with whom it has been a pleasure to share a room. These were Erik Jan de Vries, Hans de Haan, Mark de Kok and Krzysztof Wohlfeld.

Timon Idema,
August 2004